Integrated Railway Timetable Rescheduling and Dynamic Passenger Routing During a Complete Blockage

Shuguang Zhan[1,2,3], S. C. Wong[2], Pan Shang[4,*], Qiyuan Peng[1,3], Jiemin Xie[2], S. M. Lo[5]

[1] *School of Transportation and Logistics, Southwest Jiaotong University, Chengdu 610031, Sichuan, China*
shuguangzhan@my.swjtu.edu.cn, qiyuan-peng@swjtu.edu.cn

[2] *Department of Civil Engineering, The University of Hong Kong, Pokfulam, Hong Kong*
hhecwsc@hku.hk; jiemin@connect.hku.hk

[3] *National United Engineering Laboratory of Integrated and Intelligent Transportation, Southwest Jiaotong University, Chengdu, Sichuan, China*

[4] *School of Traffic and Transportation, Beijing Jiaotong University, Beijing 100044, China*
shangpan@bjtu.edu.cn

[5] *Department of Architecture and Civil Engineering, City University of Hong Kong, Kowloon, Hong Kong*
bcsmli@cityu.edu.hk

Abstract

Trains normally run as scheduled in a non-disrupted situation. However, due to external and/or internal factors, trains may deviate from their original timetable during daily operations. To this end, the involved dispatchers are required to reschedule disrupted trains to efficiently transport delayed passengers to their destinations as soon as possible. In this study, we focus on train rescheduling in a seriously disrupted situation where a track segment is completely blocked for a relatively long period of time, e.g., two hours. In this situation, trains cannot pass the disrupted segment, meaning that passengers will be unable to travel as scheduled. We simultaneously rescheduled trains and passenger routes from both the operator's and passengers' perspectives. This integrated train rescheduling and passenger rerouting problem was formulated with an Integer Linear Programming model based on a space-time network. We decomposed the integrated model into two subproblems, a train rescheduling problem and a passenger routing problem, using the alternating direction method of multipliers (ADMM) algorithm. Both subproblems could be further decomposed into a series of shortest path problems for trains or passengers, and solved by a dynamic programming algorithm. Finally, we tested our models and algorithms on both a small hypothetical railway network and a part of the Chinese high-speed railway network.

Keywords: High-speed railway; Train rescheduling; Track blockage; Integer linear programming; Alternating direction method of multipliers

1 Introduction

Advanced train control systems ensure that trains run as scheduled (according to the original timetable) in a non-disrupted situation. However, some external and internal factors, e.g., adverse weather and malfunctioning of railway infrastructure, may cause trains to deviate from their original timetable in daily operations. To minimize delays,

disrupted trains need to be rescheduled immediately after the disruption occurs. This research focuses on train rescheduling in an extremely disrupted situation where both tracks of a double-track segment are temporarily blocked. In such a situation, no train can pass the blocked double-track segment.

Two train-rescheduling strategies are utilized to manage the disrupted trains when a complete blockage occurs. One strategy is to stop the disrupted trains at intermediate stations ahead of the blocked segment and wait until the segment is cleared, and then allow the trains to continue their journey. We call this the Disrupted Trains Waiting Strategy (DTWS). The other strategy is to short-turn trains into the appropriate stations adjacent to the blocked segment before their arrival at this point. We call this the Disrupted Trains Short-turning Strategy (DTSTS). The DTWS is used on some Chinese and Japanese high-speed railways; see Zhan et al (2015) and Hirai et al (2009) for instance. The DTSTS is applied on the railway systems in some European countries, such as the Netherlands; see Nielsen et al (2012), Louwerse and Huisman (2013), Veelenturf et al (2016), Ghaemi et al (2016, 2017, 2018) and Zhu and Goverde (2019b).

Our research focuses on the DTWS, and as discussed in Zhan et al (2015), the key aspects to be determined in this strategy are the arrival and departure times for trains, the departure order of trains in each station, the intermediate stations where trains should wait for the disruption to clear, and whether it is necessary to cancel some trains. Most research has investigated rescheduling trains from the operator's point of view, i.e., with the objective of minimizing the deviation and cancellation of trains. However, minimizing the deviation of trains does not guarantee that the disposition timetable will be convenient for disrupted passengers. For example, if the number of passengers on train t_1 is 200, and that on train t_2 is 400, it is obvious that priority should be given to train t_2 to minimize the total passenger travel cost. In other words, reducing the impact of disruptions on passengers should be the primary aim of train rescheduling during a disruption. Accordingly, unlike Zhan et al (2015) and Veelenturf et al (2016), we not only considered the train delay and cancelation from the operator's point of view but also took into account the inconvenience to passengers.

An integer linear programming (ILP) model based on a space-time network was formulated to simultaneously reschedule trains and optimize passenger route-choice on a high-speed railway network. As the integrated ILP model is difficult to solve for large-scale real-world problems, we used the alternating direction method of multipliers algorithm (hereafter ADMM) to decompose the integrated model into two subproblems, a train rescheduling problem and a passenger routing problem. To ensure the feasibility of the train rescheduling subproblem, ADMM was further applied to manage the headway constraint and station capacity constraint. To this end, the train-rescheduling subproblem was further decomposed into a series of shortest path searching problems on the train space-time network, with one problem for each train. Similarly, passenger routing problem was further decomposed into a series of shortest path searching problems on the passenger space-time network, with one problem for each passenger group. *A passenger group denoted passengers that booked the same train to directly travel from the same origin station to the same destination station. If passengers had a planned transfer, we split them into two different groups, one before the transfer and the other after the transfer.* Then, a dynamic programming algorithm was applied to solve the shortest path subproblems. We tested our model and algorithm both on a small hypothetical railway network and on a part of the Chinese high-speed railway network.

Our study makes three main contributions to railway scheduling. First, we extended the problem investigated by Zhan et al (2015) to include the station track-assignment (i.e., conducting detailed train-routing at the station area) and passenger route choice. Zhan et al (2015) applied a mixed integer linear programming model to solve only the train rescheduling problem in a major disruption. However, our current model allowed us to reschedule trains and optimize passenger route choice simultaneously in very high detail, which makes our solution more practical for dispatchers. We considered the capacity allocation of platforms in a station, and examined at a microscopic level the detailed routes

used by a train to enter and leave a specific station track in the station area. Second, we used ADMM to decompose the integrated train rescheduling and dynamic passenger routing problem into several easy-to-solve subproblems, which increased the feasibility of the train schedule obtained in the lower bound solution. Finally, we tested our approach on a part of the Chinese high-speed railway network, and confirmed that our decomposition approach could solve large problems in reasonable time, unlike the CPLEX optimization program (IBM).

The remainder of this paper is organized as follows. Section 2 reviews the related literature. In Section 3, we briefly describe our problem. Model formulations for the integrated train rescheduling and passenger routing problem are given in Section 4. In Section 5, we decompose our integrated model by the ADMM algorithm and Lagrangian relaxation algorithm, and describe the related algorithms used to solve the relaxed problems. Section 6 presents the computational results. Finally, we conclude this study and discuss some future research directions in Section 7.

2 Literature review

During railway operations, a timetable is loaded in the railway dispatching center, and trains run according to this timetable in a non-disrupted situation. However, disruptions inevitably occur in daily operations and these disruptions require trains to deviate from the original timetable. Rescheduling trains in a disrupted situation is an important task for dispatchers. Several previous studies focused on train rescheduling problems, such as the recent surveys by Cacchiani et al (2014), Corman and Meng (2015) and Fang et al (2015).

In the following section, we focus on the most relevant research about train rescheduling during a blockage. During both partial and complete blockages, disrupted trains cannot pass the blocked segment as scheduled. Nielsen et al (2012) studied the rescheduling of rolling-stock in a seriously disrupted situation on the Dutch railway. They had to determine the rolling-stock connection between short-turning trains in opposite directions at short-turning stations. Louwerse and Huisman (2013) formulated the train rescheduling problem using an integer programming model, which generated a disposition timetable for a Dutch railway line. To manage the transition from the original timetable to a disposition timetable and vice versa, Veelenturf et al (2016) extended the model of Louwerse and Huisman (2013) by taking the rolling-stock rescheduling into account. Dollevoet et al (2017) integrated the timetable rescheduling, rolling-stock rescheduling and crew rescheduling, and applied an iterative approach to solve for all three in a closed loop. In a disrupted situation where both/all tracks in a segment are blocked (i.e., a complete blockage), disrupted trains are short-turned at the stations before the disrupted location, as described in Ghaemi et al (2016). These researchers focused on how to short-turn trains in multiple stations adjacent to the disrupted segment during the disruption. However, they only considered trains in one direction, and trains were only rescheduled during the disruption, with no consideration given to the transition phase. Ghaemi et al (2018) extended the work of Ghaemi et al (2016) by considering the trains in both directions and the transition phase. In a more recent research, Zhu and Goverde (2019b) further investigated how to short-turn trains when more flexible short-turn stations were available. In the research by Nielsen et al (2012), Louwerse and Huisman (2013), Veelenturf et al (2016), Dollevoet et al (2017), Ghaemi et al (2016, 2018) and Zhu and Goverde (2019b), disrupted trains were short-turned during a disruption due to track blockage. This strategy is normally used on railways where a seat reservation system is not applied.

However, in some railway systems, a seat reservation system exists. Therefore, allowing passengers to change trains is more complicated. Usually passengers have to change their booked tickets to those for the rerouted train before they board this train. In addition, they may be unable to find a seat on the re-routed train if the train does not have enough capacity. Thus, for the passengers' convenience, disrupted trains are stopped and kept at intermediate stations for the duration of the disruption instead of being short-turned, to avoid the need for passengers to transfer trains. However, passengers may need to wait for a longer time and arrive at their destination later in a waiting strategy than

with a short-turning strategy. A trade-off exists between these two strategies. Hirai et al (2009) conducted research on how to stop disrupted trains at appropriate stations during a completely blocked situation, a strategy that is called train stop deployment planning. However, they did not account for the train rescheduling required after the disruption was over. In contrast, Zhan et al (2015) considered train rescheduling both during and after the disruption, using a mixed integer linear programming model to determine the optimal way to stop disrupted trains during the disruption and how to reschedule trains after the disruption. Meng and Zhou (2011) have studied the "meet and pass" plan in a stochastic environment for trains on a single-track railway line during a temporary track blockage.

Most of these studies focused on train rescheduling from the railway operator's perspective, and thus only considered deviations, such as total train delay, weighted train delay and train cancelation. Thus, the effect of a disruption on passengers was not explicitly considered, although it is an important factor in the railway transportation system. Similarly, relatively few studies have considered passenger choice. Cadarso et al (2013) examined the passenger demand change during a disrupted situation in a rapid transit network. They rescheduled trains based on the forecast demand after the disruption occurred. However, they obtained passengers' preferences before the disposition timetable was released, and passengers therefore did not know the full range of options before making their choice. Therefore, there was insufficient interaction between the passenger demand and the disposition timetable. Gao et al (2016) rescheduled metro trains in an overcrowded condition after a disruption. Considering that large numbers of passengers would be stranded at stations due to the disruption, they introduced a skip-stop strategy to reduce the passengers' total waiting time. However, they only rescheduled trains after the end of the disruption for the recovery stage. Kroon et al (2015) rescheduled railway rolling-stock by considering the dynamic passenger demand in an iterative process with the rescheduled timetable as an input. Thus, they first rescheduled the rolling-stock based on the given timetable, and then assigned passengers to trains. To meet any outstanding passenger demand, rolling-stock was rescheduled again while the rolling-stock cost was minimized. Wagenaar et al (2017) investigated a problem similar to that in Kroon et al (2015) by accounting for dead-heading trips. The inclusion of dead-heading trips in a major disruption could help to reduce the number of trips canceled due to the lack of rolling stock. Therefore, the passenger service quality could be improved. Veelenturf et al (2017) extended the work of Kroon et al (2015) by considering timetable rescheduling, and thus iteratively solved timetable rescheduling, rolling-stock rescheduling, and passenger-assignment problems. However, they considered only train stop pattern changes made during the timetable adjustment stage, and other rescheduling strategies were not examined. Furthermore, passenger route-choice in a disrupted situation has not been well characterized. Zhu and Goverde (2019a) investigated the details of passenger-routing in a disruption by applying a simulation method based on an event-activity network. However, they only simulated the passenger route choice and assumed that the disposition timetable was provided to passengers. In a similar manner, Binder et al (2017a) studied the capacitated passenger assignment problem with various priority rules, which could be applied in passenger-centric train timetabling or rescheduling. Binder et al (2017b) more accurately studied train rescheduling and passenger route-choice in a disruption by simultaneously examining both parameters by an ILP model. However, their model was solved with CPLEX, which is a time-consuming method for solving a real-world problem; in their case study on part of the Dutch railway network, approximately 1 hour was needed to obtain a solution with an acceptable optimality gap. Therefore, they concluded that more efficient algorithms were necessary for their model to be applicable to real-world problems. In addition, Binder et al (2017b) used a 5-minute time unit to maintain the headway for trains using a segment track or station track to move in the same direction. That is, it was not necessary to consider a headway constraint because a 5-minute time unit was enough to ensure the headway. However, a five-minute time unit is not suitable for high-speed railways with a high speed and a three-minute headway. Finally, because in our work, we rescheduled trains based on the strategy of stopping disrupted trains to wait at intermediate stations for the blockage to clear, the station capacity constraint was very important (Zhan et al (2015)). This was not a critical aspect in

Binder et al (2017b) because they instead opted to short-turn trains during the disruption.

As Binder et al (2017b) mentioned, the train rescheduling and passenger routing problem is rather difficult to solve fully with CPLEX. Thus, a decomposition approach is a promising alternative that reduces the computational time required to solve such large problems. For the train rescheduling (dispatching) problem, Lamorgese and Mannino (2015) and Lamorgese et al (2016) applied a Benders-like decomposition approach to decompose the train dispatching (rescheduling) problem into a master problem associated with the line and a slave problem associated with stations. A good solution could be obtained via iterative solution of the master and slave subproblems. Lagrangian relaxation (LR) is also widely applied to solve train scheduling and rescheduling problems. Caprara et al (2002), Cacchiani et al (2012) and Zhou and Teng (2016) all used LR to decompose train-scheduling problems, while Meng and Zhou (2014) and Yin et al (2016) applied LR to solve the train-rescheduling problem. In terms of the integrated train rescheduling and passenger routing problem, Corman et al (2017) studied the microscopic delay management problem by integrating the passenger routing into a microscopic train rescheduling model in a small disruption. They introduced various heuristics to decompose the integrated model and found that good solutions could be obtained in an acceptable computational time. However, because they focused on small disruptions, train cancelation was not considered. Furthermore, they assumed that the train capacity was infinite, which is not practical in a disrupted situation. To our knowledge, LR has not been used to solve integrated train rescheduling and passenger routing on high-speed railways. However, this approach has been used to solve similar problems in airline transportation, e.g., Yan and Tseng (2002) applied LR to solve flight-scheduling and passenger-routing problems. Yet, although LR can help to decompose a large problem into subproblems, sometimes this technique affords a bad lower bound, meaning that feasibility is difficult to achieve. In this context, ADMM can be utilized to enhance the feasibility of the decomposed problem by adding a quadratic penalty term. For more information on the theory and application of ADMM, interested readers are referred to Boyd et al (2011). Recently, ADMM has been applied by Yao et al (2019) to a vehicle routing problem to improve primal and dual solution quality. Zhang et al (2019) also used ADMM to relax the headway constraint in train scheduling.

3 Problem description

We focused our study on a double-track high-speed railway network with one track in each segment for trains running in one direction. Therefore, trains running in one direction do not interact with trains running in the opposite direction in a segment between two successive stations. We assume that the tracks in a station that can be used by trains in one direction are given. Usually this is decided by some practical rules in daily operations. Passengers who travel on the high-speed railway network book tickets in advance. Therefore, they have used a seat reservation system to plan the trains to take during their journey. In a disrupted situation in which both tracks in a segment are completely blocked for a relatively long period of time, e.g., two hours, neither trains nor passengers can run as scheduled. Thus, we had to reschedule disrupted trains and routes for effected passengers immediately and efficiently to both minimize the additional operational cost to railway companies and the travel cost to passengers. In the following section, we explain the train-rescheduling problem and passenger-routing problem in detail.

3.1 Train rescheduling

During a full track blockage situation, trains cannot pass through the disrupted segment. Therefore, many trains will have to deviate from their original timetable, especially on a large and busy railway network. In such a scenario, the dispatchers must reschedule disrupted trains efficiently based on the existing capacity of the railway infrastructure and the status of traffic. Specifically, they must decide the optimal sequence, departure and arrival times of trains for each station, and whether any train cancellations are necessary. As mentioned above, we focused on a rescheduling

strategy in which disrupted trains were instructed to stop and wait at intermediate stations located before the blockage until the blockage cleared. Thus, dispatchers are also required to decide which trains should stop and wait at which stations to both prevent hindrance to other trains and to minimize a given train's operating cost. According to Chinese high-speed railway practice, trains are not allowed to be rerouted. *Therefore, rerouting trains was out of consideration in this research.* However, it was not difficult to handle train rerouting with our model with the addition of candidate rerouting routes for each train in the space-time network, although a longer computation time was sometimes needed. After all, from the perspective of railway companies, this may sometimes be the only way to minimize operational costs.

Here, we illustrate the train-rescheduling problem using the example shown in Figure 1. This example comprised a small double-track railway network with six stations (S_1 to S_6) and five segments between these stations. There were two lines: Line 1 consisted of stations S_1 to S_4, and line 2 consisted of stations S_2, S_5 and S_6. Three trains (G_1, G_2 and G_3) ran on this network: trains G_1 and G_2 ran on line 1 and train G_3 first ran on line 1 and then turned onto line 2 at station S_2. The running directions for these three trains are shown by the dotted arrow lines in Figure 1. To simplify the model, we did not include trains running in the opposite direction. We also assumed that intermediate stations S_2, S_3 and S_5 all had two tracks. We assumed a blockage occurred in the segment between stations S_2 and S_3, which meant that the dispatchers had to stop trains G_1 and G_2 at appropriate stations (S_1 and S_2) to wait for the blockage to be cleared. However, train G_3 could continue running because its route did not include the blocked location, and it was important that the two stopped trains G_1 and G_2 did not hinder train G_3. Trains G_1 and G_2 departed earlier than train G_3, and thus might hinder train G_3 if they both stopped and waited at station S_2. The dispatchers therefore had to decide which of trains G_1 and G_2 should stop at station S_2 and which should stop at station S_1. In addition, as soon as the disruption ended, they had to decide the proper sequence and time of departure for these trains. Furthermore, if there are more trains scheduled to run from station S_1 to S_4 on Line 1, the dispatchers had to decide, based on current information, whether some of these trains needed to be canceled.

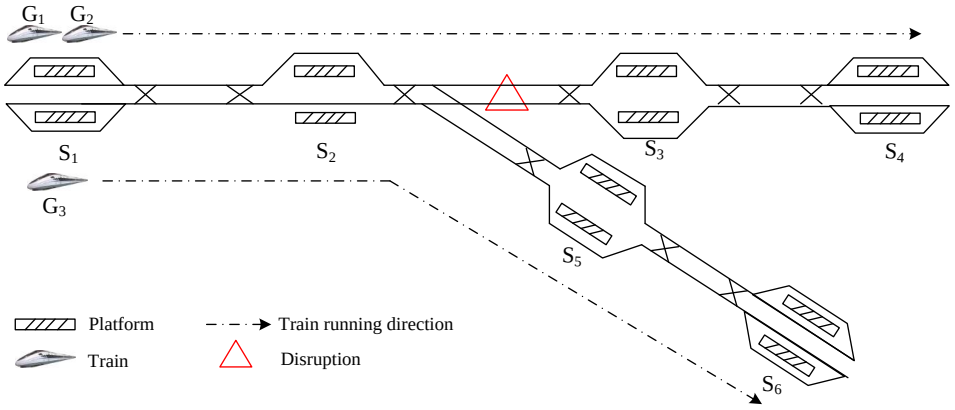

Figure 1: Train rescheduling in a complete blockage

3.2 Passenger routing

Due to the disruption, some passengers would not be able to take their scheduled train, especially for those who held tickets for canceled trains. To minimize the effect of disruptions on passengers, it would be better to allow passengers to transfer to other trains to continue their journey rather than only being able to wait for the blocked train that they booked, even though their booked train is not canceled. In principle, passengers tend to have a temporary transfer in two situations with a seat reservation: a) their reserved trains are canceled; or (b) they can arrive at their destination much earlier than by waiting for the reserved train even if the transfer time and probable changing-ticket time are

taken into account. For passengers' convenience, the passenger delay and number of passengers who cannot board any train should be minimized. Therefore, we allocated some passengers to other trains to ensure they reached their destinations in a timely fashion. However, due to the cancelation of trains and the capacity limitation of a train, some passengers could possibly not board any train, and thus would have to leave the railway system. We gave an artificial path to these rejected passengers, and a relatively high penalty, i.e., the time horizon T was added if an artificial path was utilized.

In this research, we aimed to minimize the total general passenger travel cost. There were a set of candidate paths allocated to each passenger from his/her origin o to his/her destination d, where a path was a sequence of boarding, driving, waiting, transfer and alighting movements. We introduced a utility function with each alternative path, and we assumed that the passengers selected the path with the highest utility as possible. The utility function of each path p depended on the attributes below, based on Robenek et al (2016). Given the fact that it was unusual for passengers to depart from their origin earlier than the planned time, earlier departures were not considered. The attributes were as follows:

- *In-Vehicle Time (VT_p)*: time (min) that was spent by passengers in one or several trains along their path p.
- *Waiting Time (WT_p)*: time spent (min) waiting by passengers between two consecutive trains in a station along their path p. The time that passengers spent waiting for the first train at their origin was not included as this time was accounted for by a later departure time t.
- *Number of Transfers (NT_p)*: number of times that passengers had to change trains along path p.
- *Late Departure ($LD_p = max(0, t - t_o)$)*: time difference (min) between the actual departure time t and passengers' desired departure time (t_o) from their origin o.

In a disrupted situation, passengers do not necessarily need to pay an extra fee if they change trains. Thus, we assumed that the price of a trip is equal among all the paths from the same origin-destination pair, which meant that it was unnecessary to consider fees in the utility function. For passengers who chose to travel from o by p to reach their destination, the utility function was as follows (Equation (1)):

$$U_p = -(VT_p + \beta_1 \times WT_p + \beta_2 \times NT_p + \beta_3 \times LD_p) \tag{1}$$

where β_1 to β_3 are the weights for each type of time component described above, and were used to change any other times into in-vehicle time. This utility function determines how to calculate the cost of a passenger group using a path in this study.

4 Model formulation

Some assumptions and notations are given in Section 4.1. We then introduce the space-time networks for trains and passengers in Section 4.2. In Section 4.3, we illustrate some rules used when constructing the space-time network. We define the incompatible arc sets for our model in Section 4.4. Finally, the ILP model is introduced in Section 4.5.

4.1 Assumptions and notations

To formulate the passenger-oriented train rescheduling problem, the basic assumptions were as follows:

- Each station track connected with the inbound and outbound main lines. The tracks in a station that could be used by inbound or outbound trains were defined.

- Trains that had already entered the blocked segment at the time of the disruption could continue their journey during the disruption, and the duration of the disruption was known when it occurred.
- In a given segment, inbound trains operated only on the inbound track, while outbound trains operated only on the outbound track.
- Passenger OD demands do not change due to the disruption. In addition, passengers have perfect knowledge of the future once the disruption occurs, and they comply with the advice of the railway managers.
- No crowding can occur due to the ticket reservation system.
- The rolling stock circulation is not considered.
- The time required for passengers to temporarily transfer from a preceding train to a successor train during a disruption is long when there are seat reservations due to possible ticket changes. We assume that this minimum required transfer time is given.

The notations that were used in our space-time network construction and ILP model formulation are listed in Table 1.

Table 1: The notation used in the space-time network-based model

Notations	Description
Sets:	
T	The set of times, $t, t', \tau, \tau' \in T$
N	The set of physical points, $i, i', j, j' \in N$
$N^k \subset N$	The set of physical points available for train k
$N^p \subset N$	The set of physical points available for passenger group p
F	The set of station tracks, $f \in F$
L	The set of physical links connecting two neighboring physical points, $(i,j) \in L$
K	The set of train services, $k \in K$
P	The set of passenger groups, $p \in P$
$P^k \subset P$	The set of passenger groups including passengers booked train k, $p \in P^k$
E_{tr}	The set of time-expanded train nodes, $(i,t) \in E_{tr}$
$E_{tr}^k \subset E_{tr}$	The set of time-expanded train nodes available for train k, $(i,t) \in E_{tr}^k$
E_{pa}	The set of time-expanded passenger nodes, $(i,t) \in E_{pa}$
$E_{pa}^p \subset E_{pa}$	The set of time-expanded passenger nodes available for passenger group p, $(i,t) \in E_{pa}^p$
A_{tr}	The set of time-expanded train arcs, $(i,j,t,t') \in A_{tr}$
$A_{tr}^k \subset A_{tr}$	The set of time-expanded train arcs available for train k
A_{pa}	The set of time-expanded passenger arcs, $(i,j,t,t') \in A_{pa}$
A_{pa}^p	The set of time-expanded passenger arcs available for passenger group p
$\tilde{A}_{tr}$	The set of time-expanded virtual train arcs, $(i,j,t,t') \in \tilde{A}_{tr}$
$\tilde{A}_{pa}$	The set of time-expanded virtual passenger arcs, $(i,j,t,t') \in \tilde{A}_{pa}$
$A_{tr,i}^{k,+} \subset A_{tr}^k$	The set of available arcs of train $k \in K$ leaving physical point $i \in N^k$
$A_{tr,i}^{k,-} \subset A_{tr}^k$	The set of available arcs of train $k \in K$ entering physical point $i \in N^k$
$A_{pa,i}^{p,+} \subset A_{pa}^p$	The set of available arcs of passenger group $p \in P$ leaving physical point $i \in N^p$
$A_{pa,i}^{p,-} \subset A_{pa}^p$	The set of available arcs of passenger group $p \in P$ entering physical point $i \in N^p$
$\Omega_{(i,j,t,t')} \subset A_{tr}$	The set of conflict train drive arcs with drive arc (i,j,t,t') in a segment
$\Omega'_{(i,j,t,t')} \subset A_{tr}$	The set of conflict train arcs with arc (i,j,t,t') corresponding to a station track
Parameters:	
$\hat{T}$	The end time of the planned time horizon
$c_{i,j,t,t'}^p$	The passenger travel cost on passenger arc $(i,j,t,t') \in A_{pa}$ for passenger group p
$c_{i,j,t,t'}^k$	The train operation cost on train arc $(i,j,t,t') \in A_{tr}$ for train k
n_p	The number of passengers for passenger group p
o_k	The origin of train k
d_k	The destination of train k
o'_p	The origin of passenger group p
d'_p	The destination of passenger group p
e_k	The earliest departure time of train k from its origin
l_k	The latest arrival time of train k at its destination
e'_p	The earliest departure time of passenger group p from its origin
l'_p	The latest arrival time of passenger group p at its destination
q_k	The capacity of train k
ω	The weight for train operation cost
H_{dis}^{start}	The start time of a disruption
H_{dis}^{end}	The end time of a disruption
h_{dep}^{min}	The minimum departure headway of two trains in a segment
h_{arr}^{min}	The minimum arrival headway of two trains in a segment
$h_{station}^{min}$	The minimum headway of two trains using the same station track

4.2 The space-time graph

To formulate our problem, we extended the physical railway network into two space-time networks: one being a train space-time network and the other being a passenger space-time network. In this subsection, we will first introduce the physical railway network, and then the space-time networks for trains and passengers.

4.2.1 The railway network

The railway network consisted of stations and segments spanning the area between two neighbouring stations. We focused on a double-track high-speed railway, in which each segment had two tracks. However, a station may have many tracks. A simple railway network is shown in Figure 1. Usually stations are regarded as points and segments are regarded as links, but to capture the details of the train-running and passenger-traveling process, we modeled a railway network at a more detailed level. Thus, each station with two tracks had six points and six links. A simple railway network consisting of two stations and one segment between them is given in Figure 2. We focused on one direction for this line (from station S_1 to station S_2). This physical railway network was denoted as $G = (N, L)$. In this network, the entry point and the exit point indicated the start point and end point of a station, respectively, while the start point and end point on each station track indicated the points that a station track started and ended, respectively, with these locations being where a train could pass other trains, or wait.

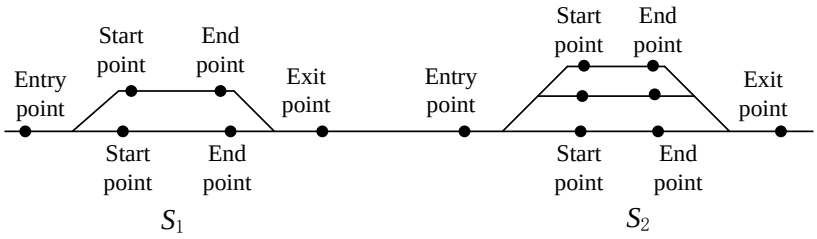

Figure 2: A simple physical railway network

4.2.2 Train space-time network

We first discretized time into intervals, i.e., $T = \{0, \sigma, 2\sigma, ..., n\sigma\}$. The selection of time interval σ was important, and could be, for example, one minute or 30 seconds; in this research, one minute was used. We add the time dimension to the physical railway network $G = (N, L)$ to extend it to a space-time network for trains, $G_{tr} = (E_{tr}, A_{tr})$, where E_{tr} was the set of time-expanded nodes of physical points N available for trains and A_{tr} was the set of time-expanded arcs of physical link L for trains. A time-expanded train arc $(i, j, t, t') \in A_{tr}$ indicated that a train began to use point i at time t and ended by using point j at time t'.

We assume that each train k started from its origin point o_k and ended at its destination point d_k, and its earliest start time from the origin and latest arrival time at its destination were e_k and l_k, respectively. Due to the disruption, some trains may not operate at all considering the limited railway capacity and the number of passengers who have booked passage on the trains. That is, it was assumed to be likely that the railway dispatchers would cancel several trains if most of the booked passengers could transfer to other running trains, as this would minimize both use of railway capacity and the train operation cost. To account for this situation, we constructed an artificial arc from a train's origin to its destination at exactly the planned time to denote that this train is canceled. The artificial train arc set was $\tilde{A}_{tr}$, and the artificial arc for train k was (o_k, d_k, e_k, l_k), $(o_k, d_k, e_k, l_k) \in \tilde{A}_{tr}$.

Based on the physical railway network and the concept of space-time network for trains, the following types of arcs representing all feasible movements of trains are defined. We used the physical network in which a train k runs from station S_1 to station S_2 in Figure 2 as an example to explain all possible space-time train arcs. To explain all the train space-time arcs, a simple example of two trains and three stations is shown in Figure 3.

- *Origin-hold arcs* represented a late departure, with a train waiting at its origin. These were expressed by the set $A_{tr}^{ohold} = \{(o_k, o_k, t, t+1) | (o_k, t), (o_k, t+1) \in E_{tr}, \forall t, t+1 \in T\}$. The origin-hold arc was an arc with one unit of time, e.g., one min. If a train waited for several minutes, we used several successive origin-hold arcs to denote

the waiting process.

- *Access arcs* represented a train starting from its origin (e.g., shunting yard) and traveling to the first station in the transportation system. This arc set was defined as: $A_{tr}^{access} = \{(o_k, i, t, t') | (o_k, t), (i, t') \in E_{tr}, \forall t, t' \in T\}$. Here i was the entry point of the first station that the train used, like the entry point of station S_1 in Figure 2.

- *Enter station arcs* represented a movement of a train from the entry point of a station to the start point of a track in the same station. They were expressed by the set $A_{tr}^{enter} = \{(i, i', t, t') | (i, t), (i', t') \in E_{tr}, \forall t, t' \in T\}$. For example, i was the entry point of station S_1, and i' was the start point of a station track in S_1 in Figure 2.

- *Pass arcs* represented a train passing a station without stopping for passengers to board and alight. A pass arc connected the start point i of a station track with the end point i' of the same station track, which could be expressed as: $A_{tr}^{pass} = \{(i, i', t, t') | (i, t), (i', t') \in E_{tr}, \forall t, t' \in T\}$.

- *Dwell arcs* represented trains waiting at stations for passengers to board and alight. A dwell arc connected the start point i of a station track and the end point i' of the same station track. The arc set could be expressed as: $A_{tr}^{dwell} = \{(i, i', t, t') | (i, t), (i', t') \in E_{tr}, \forall t, t' \in T\}$. Here i and i' were the start point and end point of a station track in a station, e.g., S_1 in Figure 2.

- *Extra wait arcs* represented trains waiting at a station track for a longer time than the required dwell time. An extra wait arc incorporated an extra unit of time. It represented a situation in which a train waited at the end point of a station track for one minute. We used several successive extra wait arcs to account for the situation wherein a train had to wait for several minutes. An extra wait arc set was expressed as: $A_{tr}^{ewait} = \{(i, i, t, t+1) | (i, t), (i, t+1) \in E_{tr}, \forall t, t+1 \in T\}$. Here point i was an end point as depicted in Figure 2.

- *Leave station arcs* represented a train leaving a station track from the track end point to the station exit point. A leave station arc connected the end point of a station track i to the exit point of the station i'. All these arcs were expressed by the set $A_{tr}^{leave} = \{(i, i', t, t') | (i, t), (i', t') \in E_{tr}, \forall t, t' \in T\}$.

- *Drive arcs* represented a train running in a segment. A drive arc connected the exit point of a station i to the entry point of the next station i'. They were expressed by the set $A_{tr}^{drive} = \{(i, i', t, t') | (i, t), (i', t') \in E_{tr}, \forall t, t' \in T\}$. For example, i was the exit point of station S_1, and i' was the entry point of station S_2 in Figure 2.

- *Egress arcs* represented a train leaving the last station to its destination, i.e., from its last station in the transportation system to a shunting yard. This set was expressed as: $A_{tr}^{egress} = \{(i, d_k, t, t') | (i, t), (d_k, t') \in E_{tr}, \forall t, t' \in T\}$, where i was the exit point of the last station and d_k was the destination point of train k (i.e., shunting yard).

- *Destination-hold arcs* represented a train finally arriving and stopping at the shunting yard. They were expressed by the set $A_{tr}^{dhold} = \{(d_k, d_k, t, t+1) | (d_k, t), (d_k, t+1) \in E_{tr}, \forall t, t+1 \in T\}$. The destination-hold arc was an arc with one unit of time. We used this arc to denote a train k stopping at its shunting yard at a final arrival time l_k.

- *Artificial arcs* represented a train starting from its origin at the earliest departure time and arriving at its destination at the latest arrival time. This arc set was defined as: $\tilde{A}_{tr} = \{(o_k, d_k, e_k, l_k) | \forall k \in K\}$.

Therefore, all the space-time train-arcs are $A_{tr} = A_{tr}^{ohold} \cup A_{tr}^{access} \cup A_{tr}^{enter} \cup A_{tr}^{dwell} \cup A_{tr}^{pass} \cup A_{tr}^{ewait} \cup A_{tr}^{leave} \cup A_{tr}^{drive} \cup A_{tr}^{egress} \cup A_{tr}^{dhold} \cup \tilde{A}_{tr}$. Thus, a pass arc denoted a train passing a station without stopping, a dwell arc indicated a train stopping at a station for a planned period of time, and an extra wait arc represented a train stopping at planned station and remained stopped longer than planned, due to a disruption. *Thus, the dwell arc ensured that*

a train stopped at a station for a period no shorter than the planned time (i.e., the minimum dwell time constraint was respected), and the extra wait arc allowed trains to stop at a station for longer than the planned time, which is necessary in a disruption. A train can only used a drive arc to pass a segment, which means that the running time of a train passing through a segment was fixed and that a train is not allowed to stop within a segment but only at a station. This is similar to the green wave policy evaluated in Corman et al (2009).

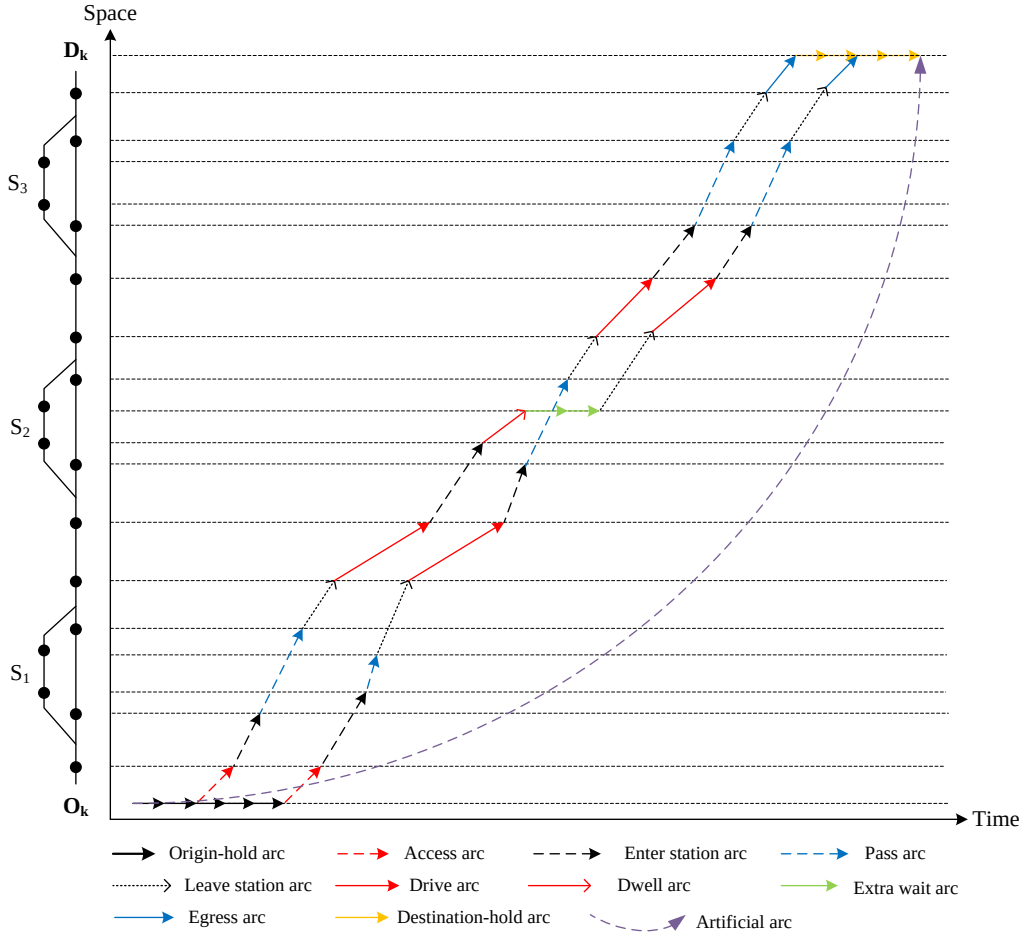

Figure 3: A simple space-time network for trains

4.2.3 Passenger space-time network

Similar to the train model, we added the time dimension to the physical railway network $G = (N, L)$ to form a space-time network for passengers $G_{pa} = (E_{pa}, A_{pa})$. Here E_{pa} was the set of time-expanded nodes of physical points N available for passengers, and A_{pa} was the set of time-expanded arcs of physical link L for passengers. A time-expanded passenger arc $(i, j, t, t') \in A_{pa}$ indicated that a passenger group began using point i at time t and ended using point j at time t'.

For each train k, there were many passengers who had booked tickets with reserved seats. As previously stated, we denoted all passengers who had booked tickets for the same train from the same origin station to the same destination station as a passenger group. Therefore, each passenger group had the same expected departure time, which was the scheduled departure time of the booked train. We did not allow a passenger group to split, as had been permitted in previous research such as Binder et al (2017b). Each passenger group p was assigned an origin point o'_p and destination point d'_p, with the earliest start and latest arrival times of e'_p and l'_p respectively. Similarly, the earliest departure time e'_p was the planned departure time of the train that passenger group p had booked. The latest arrival time l'_p was the

denoted the end of the time horizon $\hat{T}$.

Based on this space-time network for passengers, many types of arcs were used to represent the movements of passengers. Most passenger arcs were similar to the corresponding space-time train arcs except for transfer arcs and penalty arcs. The types of arcs that were used by passengers were defined as below. A simple example of three stations and one passenger group is also shown in Figure 4 to illustrate the definition of space-time passenger arcs.

- *Origin-wait arcs* represented passengers waiting at their origins. They were expressed by the set $A_{pa}^{owait} = \{(o'_p, o'_p, t, t+1) | (o'_p, t), (o'_p, t+1) \in E_{pa}, \forall t, t+1 \in T\}$. An origin-wait arc comprised one unit of time, i.e., one min. If a passenger group waited for several minutes at the origin, several successive origin-wait arcs were used to represent the waiting process.

- *Arrive arcs* represented a passenger group departing from its origin and arriving at the first station of its journey. This arc set was defined as: $A_{pa}^{arrive} = \{(o_k, i, t, t') | (o_k, t), (i, t') \in E_{pa}, \forall t, t' \in T\}$, where i was the entry point of the first station, e.g., the entry point of station S_1 in Figure 2.

- *In-platform arcs* represented a movement of passengers from the station entry point to a platform of the same station. They were expressed by the set $A_{pa}^{In-platform} = \{(i, i', t, t') | (i, t), (i', t') \in E_{pa}, \forall t, t' \in T\}$. For example, i is the entry point of station S_1, and i' is the start point of a station track in S_1 in Figure 2.

- *Pass arcs* represented passengers on a train passing a station in the middle part of their journey without stopping. A pass arc connected the start point i of a station track with the end point i' of the same station track. The set was expressed as: $A_{pa}^{pass} = \{(i, i', t, t') | (i, t), (i', t') \in E_{pa}, \forall t, t' \in T\}$. Passengers were assumed to remain in a train during a pass arc. Thus, passengers and the corresponding train were assumed to use the same arc and passengers were assumed to respect the train capacity constraint.

- *Dwell arcs* represented passengers waiting in trains at a stop station. A dwell arc connected the start point i of a station track with the end point i' of the same station track. The arc set can be expressed as: $A_{pa}^{dwell} = \{(i, i', t, t') | (i, t), (i', t') \in E_{pa}, \forall t, t' \in T\}$. As with pass arcs, passengers in a dwell arc were assumed to remain in a train, passengers and the corresponding train were assumed to use the same arc, and passengers were assumed to respect the train capacity constraint.

- *Extra wait arcs* represented passengers waiting at a station track for a longer time than the planned waiting time. An extra wait arc comprised a unit of time, which meant that passengers waited at the end point of a station track for one min. If they waited for several minutes, several extra waiting arcs were used. An extra wait arc was expressed as: $A_{pa}^{ewait} = \{(i, i, t, t+1) | (i, t), (i, t+1) \in E_{pa}, \forall t, t+1 \in T\}$, where point i represented an end point, such as in Figure 2. In this scenario, passengers could alight from the train to rest on the platform. Therefore it was not necessary for passengers to be represented by the same extra wait arc as that of corresponding trains.

- *Transfer arcs* represented passengers transferring from one station track to another station track at the same station in their middle journey. This set was expressed as: $A_{pa}^{transfer} = \{(i, j, t, t')) | (i, t), (j, t') \in E_{pa}, \forall t, t' \in T\}$. For example, passengers transferring from one end point i to another end point j at station S_1 in Figure 2 can be represented by a transfer arc.

- *Depart arcs* represented passengers departing from the end point of a station track to the station exit point. A depart arc connects the end point of a station track i with the exit point of the station i'. The arc set was expressed as $A_{pa}^{depart} = \{(i, i', t, t') | (i, t), (i', t') \in E_{pa}, \forall t, t' \in T\}$.

- *Drive arcs* represented passengers traveling on a segment. A drive arc connected the exit point of a station i with the entry point of the next station i'. The arc set was $A_{pa}^{drive} = \{(i, i', t, t') | (i, t), (i', t') \in E_{pa}, \forall t, t' \in T\}$. Note that passengers were required to be carried by trains in a segment. Thus passengers and the train that they took were constrained to using the same space-time arc, and the number of passengers using the train could not exceed the train's capacity.

- *Leave arcs* represented passengers leaving the last station prior to their destination. This set could be expressed as: $A_{pa}^{leave} = \{(i, d'_p, t, t') | (i, t), (d'_p, t') \in E_{pa}, \forall t, t' \in T\}$, where i was the exit point of the last station and d_k was the destination point of the passengers.

- *End arcs* represented passengers finally arriving at their destination and ending their whole trip at the latest arrival time. They were expressed by the set $A_{pa}^{end} = \{(d'_p, d'_p, t, t+1) | (d'_p, t), (d'_p, t+1) \in E_{pa}, \forall t, t+1 \in T\}$. The end arc comprised of one unit of time. We used this arc to denote the passengers waiting at their destination until the final arrival time l'_p. Note that the passengers usually arrived at their destination earlier than the given time ($\hat{T}$) in the passenger space-time network. Thus, this type of arcs represented the conclusion of the passengers' whole journey.

- *Penalty arcs* denoted passengers that could not travel from their origin to their destination by train due to the capacity limitation. This set was expressed as: $A_{pa}^{penalty} = \{(o'_p, d'_p, e'_p, l'_p) | (o'_p, e'_p), (d'_p, l'_p) \in E_{pa}\}$. In a penalty arc, the passenger group p was assumed to use a virtual train to travel from the origin to its destination.

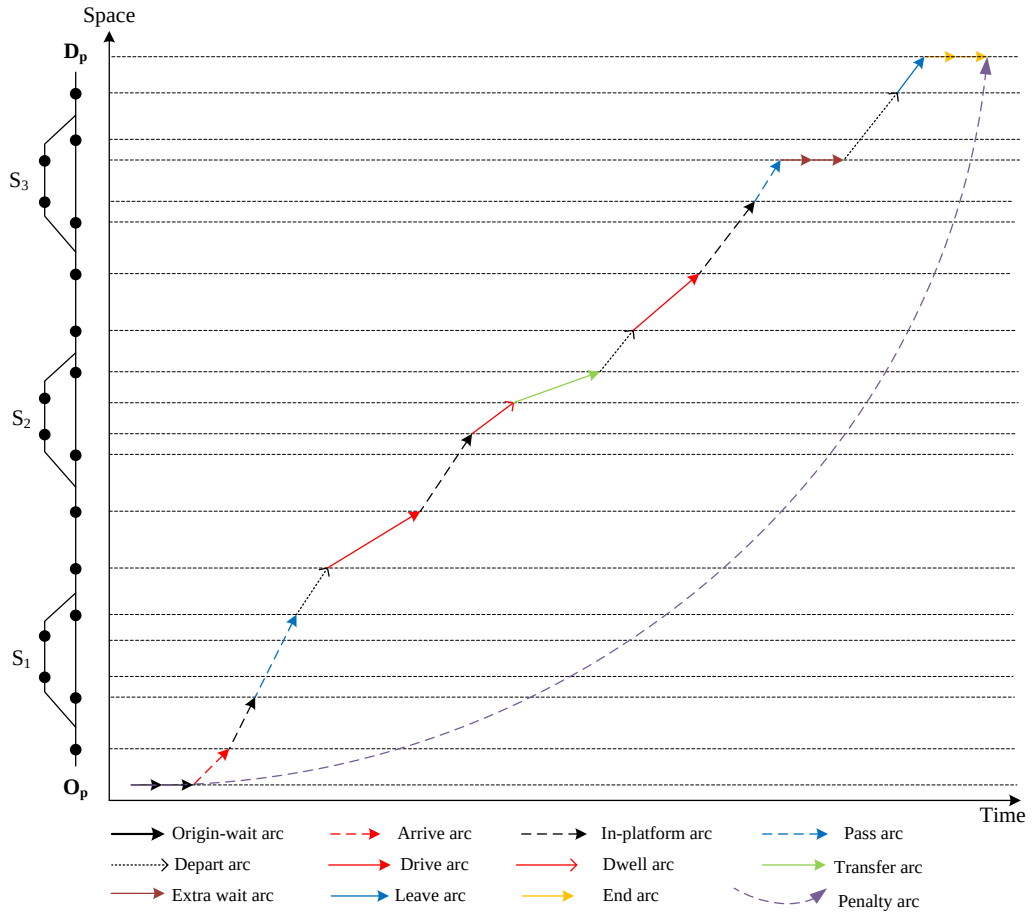

Figure 4: A simple space-time network for passengers

All the space-time passenger arcs were $A_{pa} = A_{pa}^{owait} \cup A_{pa}^{arrive} \cup A_{pa}^{In-platform} \cup A_{pa}^{pass} \cup A_{pa}^{dwell} \cup A_{pa}^{ewait} \cup A_{pa}^{transfer} \cup$

$A_{pa}^{depart} \cup A_{pa}^{drive} \cup A_{pa}^{leave} \cup A_{pa}^{end} \cup A_{pa}^{penalty}$. *Note that a drive arc, pass arc and dwell arc were for both trains and passengers because passengers were on trains on these arcs. That is, arcs of these three types belonged to* $A_{tr} \cap A_{pa}$.

4.2.4 Cost for space-time network arcs of trains and passengers

The cost for trains using an arc $a \in A_{tr}$ and for passengers using an arc $a \in A_{pa}$ was related to the arc type. During a disruption, the dispatchers expect that trains do not deviate from their origin schedule too much, and that trains can arrive at their destination as soon as possible. Therefore, we considered the cost for operating a train from its origin to the destination. We assumed that the cost of operating a train is related to the time and denoted the cost coefficient as c. In this context, an origin wait arc, which denoted the late departure of a train, and an extra wait arc, which indicated a train stopping for a longer than normal time in a station, are not desirable. Thus, we use parameters α_1 and α_2 to transfer these possibilities to a planned cost, such as scheduled dwell cost in a station. The resulting weighted arc cost of trains is shown in Table 2. Similarly, the passenger travel costs were reflected by travel time, and we used parameters β_1, β_2 and β_3 to transfer extra waiting, transfer, and late departure to basic travel time. The resulting cost for each type of weighted passenger arc is given in Table 3.

Table 2: Weighted train arc cost

Arc name	Start node	End node	Cost of train arc ($c_{ijtt'}^{k}$)
Origin-hold arcs	(o_k, t)	$(o_k, t+1)$	$\alpha_1 \times c$
Access arcs	(o_k, t)	(i, t')	0
Egress arcs	(i, t)	(d_k, t')	0
Enter station arcs	(i, t)	(j, t')	$c \times (t' - t)$
Pass arcs	(i, t)	(j, t')	$c \times (t' - t)$
Dwell arcs	(i, t)	(j, t')	$c \times (t' - t)$
Extra wait arcs	(i, t)	$(i, t+1)$	$\alpha_2 \times c$
Leave station arcs	(i, t)	(j, t')	$c \times (t' - t)$
Drive arcs	(i, t)	(j, t')	$c \times (t' - t)$
Destination-hold arcs	(d_k, t)	(d_k, t')	0
Artificial arcs	(o_k, e_k)	(d_k, l_k)	0

Table 3: Weighted passenger arc cost

Arc name	Start node	End node	Cost of passenger arc ($c_{ijtt'}^{p}$)
Origin-wait arcs	(o'_p, t)	$(o'_p, t+1)$	β_3
Arrive arcs	(o'_p, t)	(i, t')	$(t' - t)$
In-platform arcs	(i, t)	(j, t')	$(t' - t)$
Pass arcs	(i, t)	(j, t')	$(t' - t)$
Dwell arcs	(i, t)	(j, t')	$(t' - t)$
Extra wait arcs	(i, t)	$(i, t+1)$	β_1
Transfer arcs	(i, t)	(j, t')	β_2
Depart arcs	(i, t)	(j, t')	$(t' - t)$
Drive arcs	(i, t)	(j, t')	$(t' - t)$
Leave arcs	(i, t)	(d'_p, t')	0
End arcs	(d'_p, t)	$(d'_p, t+1)$	0
Penalty arc	(o'_p, e'_p)	(d'_p, l'_p)	$\hat{T}$

4.3 Basic space-time graph construction rules

In a traditional train-rescheduling problem, many operational rules must be respected, such as the minimum train running-time and dwell-time constraints. With use of the space-time graph formulation, several constraints could be

included in the space-time network construction stage (Mahmoudi and Zhou (2016), Jiang et al (2017)). These are summarized below.

(1) Train running and dwell-time constraints

The time for a train running in a segment between two stations and dwelling in a station needed to be within a given time interval. These constraints could be inherently considered when constructing the drive and wait arcs. We assumed that the running time of trains in a segment was fixed. Thus, the time $(t' - t)$ for each drive arc $(i, j, t, t') \in A_{tr}^{drive}$ was equal to the given time. Speed control is not considered in this study; interested readers are referred to Xu et al (2017) for further information about train speed control in train rescheduling. For a dwell arc $(i, j, t, t') \in A_{tr}^{dwell}$, we set its duration time $(t' - t)$ to the minimum dwell time. If a train stopped at a station for a longer time than the minimum dwell time, it used several extra wait arcs, as mentioned previously.

(2) No anticipation on the occurrence of the disruption

Before a disruption occurred, we assumed that trains were running as scheduled. That is, anticipation of the disruption was not allowed. Due to this assumption, trains had to use the same arc as scheduled before the disruption, which helped reduce the number of arcs used.

(3) Prevention of trains passing the blocked segment

No trains were permitted to pass the blocked segment during the disruption. Therefore, if a train had been scheduled to pass the segment during the disruption, it could not do so; it had to wait until the blocked segment was cleared. No train $k \in K$ could use any disrupted train arc $(i, j, t, t') \in A_{tr}$, $H_{dis}^{start} \leq t \leq H_{dis}^{end}$. Here H_{dis}^{start} and H_{dis}^{end} were the start and end time of a disruption, respectively.

4.4 Incompatible arc sets

To formulate the train rescheduling problem, we first defined an incompatible arc set $\Omega_{(i,j,t,t')}$ to model the departure and arrival headway constraints between two trains, similar to the method used by Caprara et al (2002) and Zhou et al (2017) for railway timetabling. The incompatible arc set $\Omega_{(i,j,t,t')}$ for a space-time train drive arc $(i, j, t, t') \in A_{tr}^{drive}$ was defined in Equation (2):

$$\Omega_{(i,j,t,t')} = \{(i, j, \tau, \tau') : |t - \tau| < h_{dep}^{min} \cup |t' - \tau'| < h_{arr}^{min}\} \tag{2}$$

where parameters h_{dep}^{min} and h_{arr}^{min} are the minimum departure and arrival headway time between two trains respectively. This equation indicated that if an arc $(i, j, t, t') \in A_{tr}^{drive}$ was used by a train, no other arc $(i, j, \tau, \tau') \in A_{tr}^{drive}$ with a smaller departure or arrival headway than the given value could be used again by another train. Note that if a train $k \in K$ was canceled (i.e., the artificial train arc was used), the headway constraint between this train and any other train was not required to be considered. Therefore, for any train $k \in K$, the artificial arc $(o_k, d_k, e_k, l_k) \in \tilde{A_{tr}}$ was derived from subset $\Omega_{(i,j,t,t')}$.

Similar to the incompatible arc set defined for the headway constraint, we also defined an incompatible arc set for a station track $f \in F$ to ensure that the station capacity constraint was respected in a disrupted situation. From the space-time network for trains we had constructed, we could see that possibly five arcs of different types corresponded to a station track, $(i, j, t, t') \in A_{tr}^{enter}$, $(i, j, t, t') \in A_{tr}^{pass}$, $(i, j, t, t') \in A_{tr}^{dwell}$, $(i, j, t, t') \in A_{tr}^{ewait}$, and $(i, j, t, t') \in A_{tr}^{leave}$. As each station track could in practice be used by only one train at any given time, each of these five arcs could only be occupied by one train at any given point of time. That is, these five arcs were incompatible among different trains. For each arc $(i, j, t, t') \in A_{tr}^{enter} \cup A_{tr}^{pass} \cup A_{tr}^{dwell} \cup A_{tr}^{ewait} \cup A_{tr}^{leave}$ corresponding to the same station track, its incompatible

arc set $\Omega'_{(i,j,t,t')}$ was defined as follows (Equation (3)):

$$\Omega'_{(i,j,t,t')} = \{(i',j',\tau,\tau') : (t-\tau') < h^{min}_{station} \cup (\tau - t') < h^{min}_{station}\} \tag{3}$$

where arc (i,j,t,t') and arc (i',j',τ,τ') correspond to the same station track. This indicated that if an arc (i,j,t,t') was occupied by a train, any other arc $(i',j',\tau,\tau') \in A^{enter}_{tr} \cup A^{pass}_{tr} \cup A^{dwell}_{tr} \cup A^{ewait}_{tr} \cup A^{leave}_{tr}$ could only be used by another train if it was at least $h^{min}_{station}$ minutes after arc (i,j,t,t') was released.

It is important to note that the station capacity constraint was different from the headway constraint in two aspects. One aspect was that a train could use several arcs corresponding to a station track to finish its operation within the station area. For example, a train could use a dwell arc and several extra wait arcs in the same station if it stopped at the station for a longer time than the planned dwell time. However, only one drive arc $(i,j,t,t') \in A^{drive}_{tr}$ could be used by a train in a segment. The other aspect was that a train could use an arc corresponding to a station track only after previous trains had finished using any of the five arcs corresponding to the same station track, but more than one train could simultaneously use a drive arc in a segment if their headway times were greater than the minimum headway time. *To simplify the notations in our model, we used the same format $\Phi(i,j,t,t')$ to describe the incompatible arc set for a drive arc $(i,j,t,t') \in A^{drive}_{tr}$ and an arc $(i,j,t,t') \in A^{enter}_{tr} \cup A^{pass}_{tr} \cup A^{dwell}_{tr} \cup A^{ewait}_{tr} \cup A^{leave}_{tr}$ in a station. We used A^{Strack}_{tr} to describe $A^{enter}_{tr} \cup A^{pass}_{tr} \cup A^{dwell}_{tr} \cup A^{ewait}_{tr} \cup A^{leave}_{tr}$, which included all the five arcs corresponding to a station track.*

$$\Phi(i,j,t,t') = \begin{cases} \Omega_{(i,j,t,t')} & \text{if arc } (i,j,t,t') \in A^{drive}_{tr} \\ \Omega'_{(i,j,t,t')} & \text{if arc } (i,j,t,t') \in A^{Strack}_{tr} \end{cases} \tag{4}$$

4.5 ILP model formulation

Based on the graph for trains and passengers defined in Section 4.2, and the notations defined in Table 1, we first developed the following binary variable describing trains. This variable denoted whether train k uses arc $(i,j,t,t') \in A_{tr}$, which was defined as follows.

$$x^k_{i,j,t,t'} = \begin{cases} 1 & \text{if train } k \in K \text{ uses time-expanded arc } (i,j,t,t') \in A_{tr} \\ 0 & \text{otherwise} \end{cases}$$

We also developed another binary variable to designate whether passenger group p traveled on arc $(i,j,t,t') \in A_{pa}$. Note that there are many different passenger groups $p \in P^k$ related to a given train k, because many passenger groups booked the same train k.

$$v^p_{i,j,t,t'} = \begin{cases} 1 & \text{if passenger group } p \in P \text{ uses time-expanded arc } (i,j,t,t') \in A_{pa} \\ 0 & \text{otherwise} \end{cases}$$

Passengers want to arrive at their destination as soon as possible, and we recognized this by assuming that passengers chose routes according to their utility. However, the railway operator wants to minimize the operation cost. Therefore, we took both the passenger's convenience and the train operational cost into account, and we minimized the total general travel cost for the passengers and the operation cost for the railway company.

$$\textbf{min:} \quad Z = \sum_{p \in P} \sum_{(i,j,t,t') \in A^p_{pa}} c^p_{i,j,t,t'} \times n_p \times v^p_{i,j,t,t'} + \omega \times \sum_{k \in K} \sum_{(i,j,t,t') \in A^k_{tr}} c^k_{i,j,t,t'} \times x^k_{i,j,t,t'} \tag{5}$$

subject to:

Train operational constraints:

$$\sum_{(i,j,t,t')\in A^{k,+}_{tr,o_k}} x^k_{i,j,t,t'} = 1 \quad \forall k \in K \tag{6}$$

$$\sum_{(i,j,t,t')\in A^{k,-}_{tr,i}} x^k_{i,j,t,t'} = \sum_{(j,i,t,t')\in A^{k,+}_{tr,i}} x^k_{j,i,t,t'} \quad \forall k \in K,\ \forall i \in N^k : i \neq o_k \cap i \neq d_k, \tag{7}$$

$$\sum_{(i,j,t,t')\in A^{k,-}_{tr,d_k}} x^k_{i,j,t,t'} = 1 \quad \forall k \in K \tag{8}$$

$$\sum_{k\in K} \sum_{(i',j',\tau,\tau')\in\Phi(i,j,t,t')} x^k_{i',j',\tau,\tau'} \leq 1 \quad \forall (i,j,t,t') \in A^{drive}_{tr} \text{ or } (i,j,t,t') \in A^{Strack}_{tr} \tag{9}$$

$$x^k_{i,j,t,t'} \in \{0,1\} \quad \forall (i,j,t,t') \in A_{tr}, \forall k \in K \tag{10}$$

Passenger route choice constraints:

$$\sum_{(i,j,t,t')\in A^{p,+}_{pa,o'_p}} v^p_{i,j,t,t'} = 1 \quad \forall p \in P \tag{11}$$

$$\sum_{(i,j,t,t')\in A^{p,-}_{pa,d'_p}} v^p_{i,j,t,t'} = 1 \quad \forall p \in P \tag{12}$$

$$\sum_{(i,j,t,t')\in A^{p,-}_{pa,i}} v^p_{i,j,t,t'} = \sum_{(j,i,t,t')\in A^{p,+}_{pa,i}} v^p_{j,i,t,t'} \quad \forall p \in P,\ \forall i \in N^p : i \neq o'_p \cap i \neq d'_p \tag{13}$$

$$\sum_{p\in P} n_p \times v^p_{i,j,t,t'} \leq \sum_{k\in K} q_k \times x^k_{i,j,t,t'} \quad \forall (i,j,t,t') \in A_{tr} \cap A_{pa} \tag{14}$$

$$v^p_{i,j,t,t'} \geq x^k_{i,j,t,t'} \quad \forall k \in K, \forall p \in P^k, \forall (i,j,t,t') \in A^k_{tr} \cap A^p_{pa} \tag{15}$$

$$v^p_{i,j,t,t'} \in \{0,1\} \quad \forall p \in P, \forall (i,j,t,t') \in A^p_{pa} \tag{16}$$

In objective (5), the first sum is the total general passenger travel cost, while the second sum is the total weighted train operation cost. Parameter ω denotes the relative weight of these two parts, and its value can be decided by the railway operators. The cost of a passenger group using a penalty arc is high, while that of a train using an artificial train arc is low. Therefore, during a disruption, railway managers can make a trade-off between the passenger convenience and the train operation cost. Constraints (6), (7), and (8) are the train flow conservation constraints. Constraint (9) prevents any two conflict arcs in a segment between two successive stations being occupied by trains simultaneously when arc $(i,j,t,t') \in A^{drive}_{tr}$. This is also called the headway constraint for any two trains. Constraint (9) is also the station capacity constraint when $(i,j,t,t') \in A^{Strack}_{tr}$, which formulates that at most one train can use an arc of a station track at any time t. The detailed difference between headway and station capacity constraints was explained in Section 4.4. Constraint (10) shows the domain of binary variable $x^k_{i,j,t,t'}$.

Constraints (11), (12), and (13) represent the passenger flow conservation constraints. The train capacity constraint is given by (14), which states that the total number of passengers that use arc (i,j,t,t') cannot exceed the total capacity of train k that utilizes the same arc. This constraint also indicates that if passengers choose to use arc (i,j,t,t'), at least one train must also use it. Recall that in constraint (14), we only considered drive arcs, pass arcs and dwell arcs that are used by both trains and passengers. Constraint (15) ensures that if train k is not canceled, all passengers in group p that have booked tickets for train k will keep using this train k. Note that this constraint can be relaxed if passengers are allowed to change trains freely, especially when no seat reservation system is applied. The last constraint shows the domain of variable $v^p_{i,j,t,t'}$.

Our model is similar to that in Kecman et al (2013) for the train rescheduling problem, in which train rescheduling is considered in detail, close to a microscopic level. However, the model in Kecman et al (2013) was based on an alternative

graph, and big M formulations were applied to linearize disjunctive constraints; in contrast, our model is based on space-time networks, and time-indexed formulations are applied to linearize disjunctive constraints. Furthermore, our model integrates passenger routing into train rescheduling in a major disruption; however, the models in Kecman et al (2013) only considered train rescheduling in a small disruption.

5 Problem decomposition and a solution method

To simplify the notations used in our model, we use a instead of (i, j, t, t') as the space-time arc index in the the following. In this section, we will first introduce how to decompose our model by ADMM, and then illustrate the approach to solve the decomposed problem. Finally, we introduce LR to decompose our model to obtain a lower bound.

5.1 Problem decomposition based on ADMM

Lagrangian relaxation is a widely used dual decomposition approach, that can reduce the complexity of optimization problems by relaxing the complicated constraints and adding them in the objective function. After the decomposition, the original problem usually can be divided into several easy-to-solve subproblems. Augmented Lagrangian relaxation further introduces a quadratic penalty term into the objective when a complicated constraint is relaxed. Compared to Lagrangian relaxation, Augmented Lagrangian relaxation can improve the robustness and functional convexity. However, the quadratic term in the objective function makes the relaxed problem nonlinear, and it thus cannot be easily decomposed into several independent subproblems. That is, the variables for subproblems are dependent. By combining the Augmented Lagrangian relaxation with the block coordinate decent method, ADMM was adopted to update variables sequentially in a block-by-block manner (Bertsekas (1999)). Therefore, the relaxed problem was made separable. In addition, compared to LR, ADMM has the advantages of breaking symmetry and strong convexity. Therefore, we used ADMM instead of LR to decompose our integrated model, as the lower bound provided by the latter is far from feasibility. The theoretical convergence of the standard ADMM for convex programming with two blocks has been discussed (Gabay (1983); Eckstein and Bertsekas (1992)). However, researchers have also recognized that there is no guarantee for the convergence of ADMM when extended to handle multiple blocks or when applied to nonconvex problems (Lin et al (2015); Chen et al (2016)). Due to the nature of integer variables, our proposed model is considered a type of nonconvex programming model. Furthermore, the proposed solution approach is an extended multi-block version of ADMM. In these complex situations, convergence of our ADMM-based framework cannot be guaranteed. Our approach aims to find a good feasible solution within a short computation time, but it cannot guarantee the optimal solution. For more information about ADMM, we refer the readers to Bertsekas (1999) and Boyd et al (2011), and two recent papers by Yao et al (2019) and Zhang et al (2019).

The passenger-oriented train rescheduling model described in the previous section was an ILP model. It included three types of constraints: train-routing constraints (6) $\sim$ (10) corresponding to binary variable x_a^k, passenger routing constraints (11) $\sim$ (13) and (16) corresponding to binary variable v_a^p, and coupling constraints (14) and (15) corresponding to both variables x_a^k and v_a^p. This integrated problem was quite complicated to solve by commercial solver, e.g., CPLEX. Therefore, we decomposed the integrated model by a two-level ADMM decomposition approach. In the first level, we relaxed the coupling constraint (14) to divide the integrated problem into two subproblems. Constraint (15) was to prevent passengers transferring to other trains if the train that they booked was in operation. However, as this may cause long delays for some passengers, we allowed passengers to transfer to other trains even if the train they booked was not canceled, i.e., constraint (15) was omitted. We introduced some strategies to manage this constraint in a high-speed railway system with seat reservation in our solving approach. In the second level, we relaxed the train

headway and station capacity constraint (9), as this constraint is a complicated constraint corresponding to many trains instead of a single train. This two-level decomposition procedure is shown in Figure 5, where $|K|$ and $|P|$ are the total numbers of trains and passenger groups. respectively.

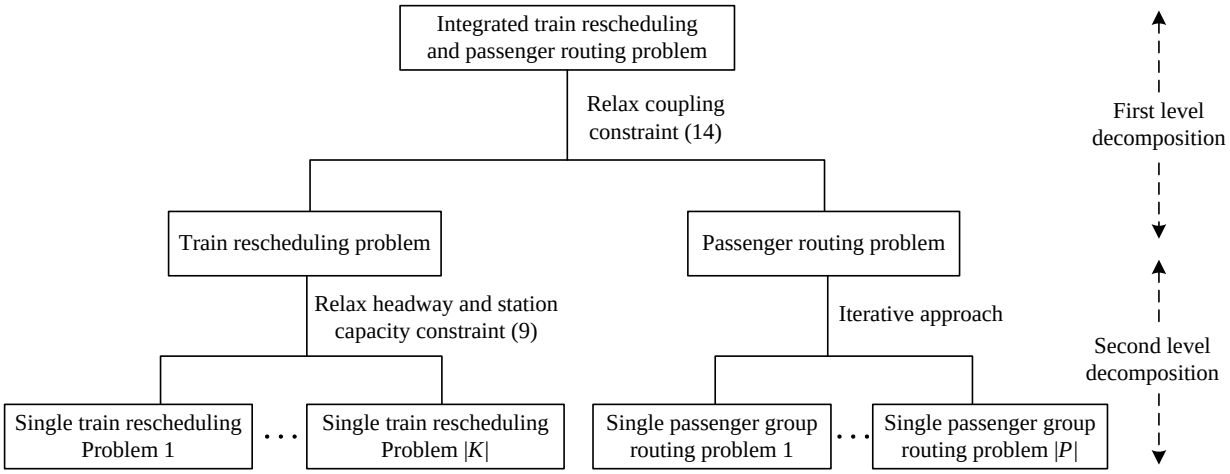

Figure 5: The two-layer decomposition procedure

To relax the two complex constraints (constraints (9) and (14)) by ADMM, we first introduce two slack variables r_a and s_a to transfer them from inequality constraints to equality constraints (9a) and (14a).

$$\sum_{k\in K}\sum_{a'\in\Phi(a))} x_{a'}^k + r_a = 1 \tag{9a}$$

$$\sum_{p\in P} n_p \times v_a^p + s_a = \sum_{k\in K} q_k \times x_a^k \tag{14a}$$

Then, we introduced two sets of Lagrangian multipliers and quadratic penalty parameters (Table 4). Parameter $\xi(a)$ is the Lagrangian multiplier corresponding to the train headway constraint and station capacity constraint, and $\gamma(a)$ is the Lagrangian multiplier related to coupling constraint (14). Parameters ρ_1 and ρ_2 are the quadratic penalty coefficients for relaxing constraints (9) and (14) respectively.

Table 4: The definitions of augmented Lagrangian multipliers

Lagrangian multipliers	Quadratic penalty	Defining ranges	Corresponding constraints
$\xi(a)$	ρ_1	$\forall a \in A_{tr}^{drive}$ or $a \in A_{tr}^{Strack}$	Constraint (9)
$\gamma(a)$	ρ_2	$\forall a \in A_{tr} \cap A_{pa}$	Constraint (14)

(1) $A_{tr}^{Strack} = A_{tr}^{enter} \cup A_{tr}^{pass} \cup A_{tr}^{dwell} \cup A_{tr}^{ewait} \cup A_{tr}^{leave}$.
(2) $A_{tr} \cap A_{pa} = A_{tr}^{drive}(A_{pa}^{drive}) \cup A_{tr}^{pass}(A_{pa}^{pass}) \cup A_{tr}^{dwell}(A_{pa}^{dwell})$.

By introducing these slack variables, Lagrangian multipliers and quadratic penalty parameters, the two constraints could be incorporated into the objective function. The relaxed model was thus as follows (Equation (17)):

$$\begin{aligned}\min \quad Z_L = &\sum_{p\in P}\sum_{a\in A_{pa}^p} c_a^p \times n_p \times v_a^p + \omega \times \sum_{k\in K}\sum_{a\in A_{tr}^k} c_a^k \times x_a^k + \\ &\sum_{a\in A_{tr}^{drive} \text{or } a\in A_{tr}^{Strack}} \xi(a)\Big(\sum_{k\in K}\sum_{a'\in\Phi(a)} x_{a'}^k - 1\Big) + \rho_1/2 \sum_{a\in A_{tr}^{drive} \text{or } a\in A_{tr}^{Strack}} \Big(\sum_{k\in K}\sum_{a'\in\Phi(a))} x_{a'}^k - 1 + r_a\Big)^2 + \\ &\sum_{a\in A_{tr}\cap A_{pa}} \gamma(a) \times \Big(\sum_{p\in P} n_p \times v_a^p - \sum_{k\in K} q_k \times x_a^k\Big) + \rho_2/2 \sum_{a\in A_{tr}\cap A_{pa}} \Big(\sum_{p\in P} n_p \times v_a^p - \sum_{k\in K} q_k \times x_a^k + s_a\Big)^2\end{aligned} \tag{17}$$

subject to (6)-(8) and (10); (11)-(13) and (16).

In the model, we had two types of variables. Thus, the relaxed model could be decomposed into two subproblems: a train rescheduling subproblem and a passenger routing subproblem. We could then iteratively solve the two subproblems by the block coordinate descent method. That is, when we solved one subproblem, we temporarily fixed the variables in the other subproblem based on the latest solution. This iterative procedure is illustrated in Figure 6, in which it can be seen that when the passenger routing problem (**Pv**) in iteration m is solved, the variable x_a^k for the train rescheduling problem was temporarily fixed in the current iteration. After we solved the passenger routing problem in iteration m, we could solve the train rescheduling problem (**Px**) in iteration $m+1$ with the variable v_a^p fixed to its value obtained in iteration m. Then, after solving the train rescheduling problem (**Px**) in iteration $m+1$, we temporarily fixed its solution and solved the passenger routing problem (**Pv**) in iteration $m+2$. We used $\overline{x}_a^k$ to denote the fixed value of variable x_a^k, and $\overline{v}_a^p$ to denote the fixed value of variable v_a^p. The two subproblems in our iterative approach were as follows (Equations (18) and (19)):

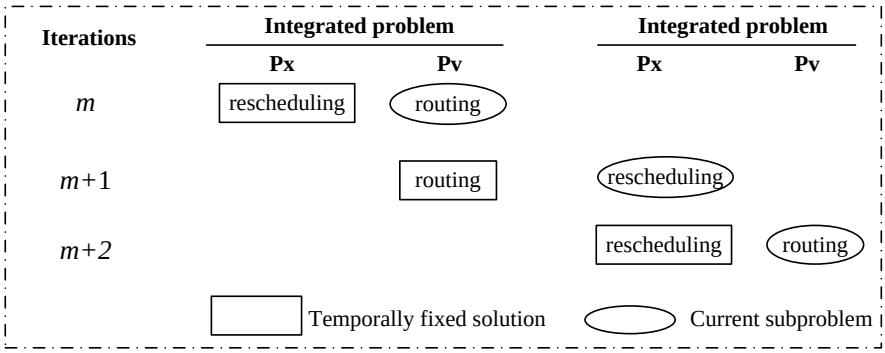

Figure 6: Procedure for iterative solution of the two subproblems.

Px:

$$\begin{aligned}\text{min:}\quad Z_x =& \omega \times \sum_{k\in K}\sum_{a\in A_{tr}^k} c_a^k \times x_a^k + \\ & \sum_{a\in A_{tr}^{drive} \text{or } a\in A_{tr}^{Strack}} \xi(a)\Big(\sum_{k\in K}\sum_{a'\in\Phi(a)} x_{a'}^k - 1\Big) + \rho_1/2 \sum_{a\in A_{tr}^{drive} \text{or } a\in A_{tr}^{Strack}} \Big(\sum_{k\in K}\sum_{a'\in\Phi(a)} x_{a'}^k - 1 + r_a\Big)^2 + \\ & \sum_{a\in A_{tr}\cap A_{pa}} \gamma(a) \times \Big(\sum_{p\in P} n_p \times \overline{v}_a^p - \sum_{k\in K} q_k \times x_a^k\Big) + \rho_2/2 \sum_{a\in A_{tr}\cap A_{pa}} \Big(\sum_{p\in P} n_p \times \overline{v}_a^p - \sum_{k\in K} q_k \times x_a^k + s_a\Big)^2\end{aligned} \tag{18}$$

subject to (6)-(8) and (10).

Pv:

$$\begin{aligned}\text{min:}\quad Z_v =& \sum_{p\in P}\sum_{a\in A_{pa}^p} c_a^p \times n_p \times v_a^p + \\ & \sum_{a\in A_{tr}\cap A_{pa}} \gamma(a) \times \Big(\sum_{p\in P} n_p \times v_a^p - \sum_{k\in K} q_k \times \overline{x}_a^k\Big) + \rho_2/2 \sum_{a\in A_{tr}\cap A_{pa}} \Big(\sum_{p\in P} n_p \times v_a^p - \sum_{k\in K} q_k \times \overline{x}_a^k + s_a\Big)^2\end{aligned} \tag{19}$$

subject to (11)$\sim$(13) and (16).

As both subproblems were composed of only flow-conservation constraints and variable-domain constraints, they could be treated as two generalized least cost/shortest path problems in a space-time network, with one problem being for trains, and the other being for passengers. The shortest path problem could be solved by, e.g., label correcting or dynamic programming (DP) in polynomial time. In this research, DP was applied to solve the shortest path subproblem.

5.2 Solution approach to the decomposed subproblems

By using the decomposition approach described in the previous section, we could derive two subproblems. However, the quadratic terms in the objectives of the two subproblems obtained by ADMM were difficult to handle. Thus, we transformed these into linear terms, given the fact that both variables in the two subproblems were binary variables. The detailed processes for working with the quadratic terms are shown in Appendix A. After transforming the quadratic term into a linear term in the objective function, the train rescheduling subproblem could be further decomposed into single-train rescheduling subproblems, and the model for a single train k was as follows (Equation (20)):

$\boldsymbol{P_x^k}$:

$$\begin{aligned}\min \quad Z_x^k =& \omega \times \sum_{a \in A_{tr}^k} c_a^k \times x_a^k + \\ & \sum_{a \in A_{tr}^{drive} \text{or } a \in A_{tr}^{Strack}} \sum_{a' \in \Phi(a)} \left[\xi(a) \times x_{a'}^k + \rho_1/2 \times (2\psi_{a'}^k - 1) \times x_{a'}^k\right] + \\ & \sum_{a \in A_{tr} \cap A_{pa}} \left[\gamma(a) \times (-q_k \times x_a^k) + \rho_2/2 \times q_k \times (q_k + 2 \times \mu_a^k - 2 \times \sum_{p \in P} n_p \times \overline{v}_a^p) \times x_a^k\right] \\ =& \sum_{a \in A_{tr}^k} \overline{c}_a^k \times x_a^k\end{aligned} \tag{20}$$

subject to constraints (6)-(8) and (10), and where $\overline{c}_a^k$ is the general cost for train k using arc a, which is defined as follows (Equation (20a)):

$$\overline{c}_a^k = \begin{cases} c_a^k & a \notin (A_{tr}^{drive} \cup A_{tr}^{Strack}) \text{ and } a \notin A_{tr} \cap A_{pa} \\ c_a^k + \xi(a) + (\rho_1 \times \psi_{a'}^k - \rho_1/2) & a \in (A_{tr}^{drive} \cup A_{tr}^{Strack}) \\ c_a^k - q_k \times \gamma(a) + \rho_2/2 \times q_k \times (q_k + 2 \times \mu_a^k - 2 \times \sum_{p \in P} n_p \times \overline{v}_a^p) & a \in A_{tr} \cap A_{pa} \\ c_a^k + \xi(a) + (\rho_1 \times \psi_{a'}^k - \rho_1/2) - q_k \times \gamma(a) + & \\ \rho_2/2 \times q_k \times (q_k + 2 \times \mu_a^k - 2 \times \sum_{p \in P} n_p \times \overline{v}_a^p) & a \in (A_{tr}^{drive} \cup A_{tr}^{Strack}) \text{ and } a \in A_{tr} \cap A_{pa} \end{cases} \tag{20a}$$

In Equation (20a), $a' \in \Phi(a)$ for $a \in (A_{tr}^{drive} \cup A_{tr}^{Strack})$. We may have two parts of linear and quadratic penalty terms because we use two-layer decomposition by ADMM. The second part is obtained by relaxing the coupling constraint (14). We can see that either the train capacity q_k or the volume of passengers (n_p) in passenger group p, is multiplied in the cost function in equation (20a), which makes the cost for relaxing the coupling constraint much higher than that for relaxing the headway and station capacity constraints. In our study, it was more important to obtain a feasible train disposition timetable than to solve the passenger routing problem because a feasible timetable was the prerequisite for passenger routing. Therefore, the cost for relaxing the coupling constraint (14) could not be higher than that for relaxing the headway and station capacity constraints (9). To satisfy this requirement, we introduced a Lagrangian heuristic to ensure the feasibility of the integrated problem. Specifically, we set an upper bound (up_1) and a lower bound (lo_1) for the cost of the linear term and an upper bound (up_2) and a lower bound (lo_2) for the quadratic term for relaxing the coupling constraint, where $up_1 + up_2 < \rho_1$, and $|lo_1| + |lo_2| < \rho_1$. This could help to limit the cost of relaxing the coupling constraint. Thus, the cost of train k using arc a becomes represented by Equation (20b) (below)

when we search for the train path by a dynamic programming algorithm:

$$\overline{c}_a^k = \begin{cases} c_a^k & a \notin (A_{tr}^{drive} \cup A_{tr}^{Strack}) \text{ and } a \notin A_{tr} \cap A_{pa} \\ c_a^k + \xi(a) + (\rho_1 \times \psi_a^k - \rho_1/2) & a \in (A_{tr}^{drive} \cup A_{tr}^{Strack}) \\ c_a^k - \max\{lo_1, \min\{q_k \times \gamma(a), up_1\}\} + \max\{lo_2, \min\{ & \\ \rho_2/2 \times q_k \times (q_k + 2 \times \mu_a^k - 2 \times \sum_{p \in P} n_p \times \overline{v}_a^p), up_2\}\} & a \in A_{tr} \cap A_{pa} \\ c_a^k + \xi(a) + (\rho_1 \times \psi_a^k - \rho_1/2) - & \\ \max\{lo_1, \min\{q_k \times \gamma(a), up_1\}\} + \max\{lo_2, \min\{ & \\ \rho_2/2 \times q_k \times (q_k + 2 \times \mu_a^k - 2 \times \sum_{p \in P} n_p \times \overline{v}_a^p), up_2\}\} & a \in (A_{tr}^{drive} \cup A_{tr}^{Strack}) \text{ and } a \in A_{tr} \cap A_{pa} \end{cases} \tag{20b}$$

Similarly, the passenger routing subproblem could also be decomposed into many single passenger-group routing subproblems after transforming the quadratic term into a linear term in Equation (19). The subproblem for each passenger group p was as follows (Equation (21)):

$\boldsymbol{P_v^p}$:

$$\begin{aligned} \min \quad Z_v^p &= \sum_{a \in A_{pa}^p} c_a^p \times n_p \times v_a^p + \\ &\quad \sum_{a \in A_{tr} \cap A_{pa}} \gamma(a) \times n_p \times v_a^p + \rho_2/2 \times n_p \times (n_p - 2 \times \sum_{k \in K} q_k \times \overline{x}_a^k + 2 \times \mu_a^p) \times v_a^p \\ &= \sum_{a \in A_{pa}^p} \overline{c}_a^p \times v_a^p \end{aligned} \tag{21}$$

subject to Equations (11)-(13) and (16).

In Equation (21), $\overline{c}_a^p$ is the general cost for passenger group p using arc a, and is defined as follows (Equation (21a)).

$$\overline{c}_a^p = \begin{cases} c_a^p \times n_p & a \notin A_{tr} \cap A_{pa} \\ c_a^p \times n_p + \gamma(a) \times n_p + \rho_2/2 \times n_p \times (n_p - 2 \times \sum_{k \in K} q_k \times \overline{x}_a^k + 2 \times \mu_a^p) & a \in A_{tr} \cap A_{pa} \end{cases} \tag{21a}$$

As mentioned previously, we omit constraint (15) of the ILP model in the problem decomposition. Here we introduce how we handle that constraint in our solution approach. We introduce a coefficient δ ($0 < \delta < 1$) of the cost to a passenger who uses his or her reserved train. If a passenger uses the reserved train, the travel cost equals the general cost multiplied by δ. That is, if passenger group p uses its reserved train to travel on arc a, the cost c_a^p in Equation (21a) equals to $\delta \times c_a^p$. In this way, we give priority to passengers who choose their reserved train in a seat reservation system.

Using the problem decomposition method described, we can solve the subproblems by a cyclic block coordination descent method (Saha and Tewari (2013) and Sun and Hong (2015)). The detailed procedure for the solution approach is given in Algorithm 1 (below). Note that an inner iteration was utilized both in Step 2.1 to solve the train-rescheduling subproblem and in Step 2.2 to solve the passenger-routing subproblem. The methods of these solutions can be found in Algorithm 2 in Appendix C and Algorithm 3 in Appendix D, respectively.

Algorithm 1 Two-layer decomposition algorithm

Input:

The space-time network $G_{tr} = (E_{tr}, A_{tr})$ for trains and $G_{pa} = (E_{pa}, A_{pa})$ for passengers;

The original timetable and passenger OD matrix;

The disruption information;

The planning horizon and the number of trains and passenger groups considered within the planning horizon

Output:

The best train trajectory in the space-time network (for train operation) for each train $k \in K$;

The passenger route choice in the space-time network (for passenger routing) for each passenger group $p \in P$

Step 1: Initialization

Initialize the iteration number $m = 0$;

Initialize Lagrangian multipliers $\xi^m(a)$ and $\gamma^m(a)$, and penalty parameter ρ_1 and ρ_2;

Initialize the upper bounds up_1 and up_2, and lower bounds lo_1 and lo_2;

Set the best upper bound $UB^* = +\infty$;

Set the maximum iteration step M;

Initialize the variable $v_a^p = 0$ for each $p \in P$ and calculate $\sum_{p \in P} n_p \times v_a^p$ as input for subproblem **Px**

Step 2: Solve the decomposed subproblems iteratively

Step 2.1: Solve subproblem Px

Calculate the generalized Lagrangian cost $\overline{c}_a^k$ for each space-time train arc a by Equation (20b);

Solve the P_x^k for each train k by forward DP (see Algorithm 2 in Appendix C);

Obtain the train rescheduling results of x_a^k and the value of the objective function Z_x^m at iteration m;

Calculate $\sum_{k \in K} x_a^k$ for each train arc a, as input for subproblem **Pv**

Step 2.2: Solve subproblem Pv

Calculate the generalized Lagrangian cost $\overline{c}_a^p$ for each space-time passenger arc a by Equation (21a);

Solve the P_v^p for each passenger group p by forward DP (see Algorithm 3 in Appendix D);

Calculate the passenger routing results of v_a^p and the value of the objective function Z_v^m at iteration m;

Calculate $\sum_{p \in P} v_a^p$ for each passenger arc a, as input for subproblem **Px** in the following iteration

Step 3: Generating upper bound UB^*

Generate a feasible solution (by Algorithm 4 in Appendix E) and calculate upper bound of the objective value at current iteration UB^m;

Generate the new best upper bound $UB^* = \min\{UB^*, UB^m\}$

Step 4: Updating the values for Lagrangian multipliers

Update Lagrangian multiplier for coupling constraint:

$\gamma(a)^{m+1} = \gamma(a)^m + \rho_2 \times (\sum_{p \in P} n_p \times v_a^p - \sum_{k \in K} q_k \times \overline{x}_a^k) \quad \forall a \in A_{tr} \cap A_{pa}$;

Note that the values of parameters ρ_1 and ρ_2 are fixed in this study

Step 5: Termination conditions

If $m < M$, let $m = m + 1$, and go back to Step 2; otherwise, output the best upper bound solution and terminate the algorithm.

5.3 Calculate the lower bound solution by LR

The ADMM-based solution framework is applied to obtain feasible solutions. To evaluate the quality of the obtained feasible solutions, we construct a pure LR model to calculate the corresponding lower bound solutions. Specifically, the quadratic penalty terms are removed from Equation (17). The LR relaxation model is as follows:

$$\begin{aligned} \min \quad Z_{LR} = & \sum_{p \in P} \sum_{a \in A_{pa}^p} c_a^p \times n_p \times v_a^p + \omega \times \sum_{k \in K} \sum_{a \in A_{tr}^k} c_a^k \times x_a^k + \\ & \sum_{a \in A_{tr}^{drive} \text{or } a \in A_{tr}^{Strack}} \xi(a) (\sum_{k \in K} \sum_{a' \in \Phi(a)} x_{a'}^k - 1) + \\ & \sum_{a \in A_{tr} \cap A_{pa}} \gamma(a) \times (\sum_{p \in P} n_p \times v_a^p - \sum_{k \in K} q_k \times x_a^k) \end{aligned} \tag{22}$$

subject to (6)-(8) and (10); (11)-(13) and (16).

Like the decomposition procedure of the ADMM-based model, the LR-based model can be decomposed into two subproblems.

$\bar{\boldsymbol{P}}_{\boldsymbol{x}}$:

$$\begin{aligned}\text{min:}\quad \bar{Z}_x =& \omega \times \sum_{k\in K}\sum_{a\in A_{tr}^k} c_a^k \times x_a^k + \\ & \sum_{a\in A_{tr}^{drive} \text{or } a\in A_{tr}^{Strack}} \xi(a)\Big(\sum_{k\in K}\sum_{a'\in\Phi(a)} x_{a'}^k - 1\Big) - \sum_{a\in A_{tr}\cap A_{pa}} \gamma(a) \times \sum_{k\in K} q_k \times x_a^k\end{aligned} \tag{23}$$

subject to (6)-(8) and (10).

$\bar{\boldsymbol{P}}_{\boldsymbol{v}}$:

$$\text{min:}\quad \bar{Z}_v = \sum_{p\in P}\sum_{a\in A_{pa}^p} c_a^p \times n_p \times v_a^p + \sum_{a\in A_{tr}\cap A_{pa}} \gamma(a) \times \sum_{p\in P} n_p \times v_a^p \tag{24}$$

subject to (11)-(13) and (16).

The dynamic programming algorithms used to solve these two subproblems $\bar{\boldsymbol{P}}_{\boldsymbol{x}}$ and $\bar{\boldsymbol{P}}_{\boldsymbol{v}}$ are similar to those in the ADMM solution procedure. The only difference is the LR cost for each train and passenger arc. We use the traditional sub-gradient method to update both multipliers $\xi(a)$ and $\gamma(a)$ in LR iterations; however, as mentioned above, the multiplier for the coupling constraint (14) is much larger than that for the headway constraint (9), so the step-size used to update $\gamma(a)$ should be smaller than that used to update $\xi(a)$. In this study, the former is $\epsilon/(1 + iteration\_step)$, where the parameter ϵ is smaller than 1 and the *iteration_step* is the current iteration step in LR; the latter is $1/(1 + iteration\_step)$. The detailed iterative procedure of LR is well known; thus, we omit it here.

6 Experiments and results

In this section, we describe the experimental results from using our approach on an artificial railway network and part of the real-world Chinese high-speed railway network. In the small case study, the model was coded in Python, and IBM ILOG CPLEX 12.8 was utilized as the solver with CPLEX parameters set to their default values. In the large case study, our algorithm was coded in Python. The small case study were run on an Intel Core i7-7700 processor CPU @3.60GHz (i.e., 3.60GHz, 16.0GB RAM desktop), and the large case study were run on an Intel Core i9-9900K processor CPU @3.60GHz (i.e., 3.60GHz, 32.0GB RAM desktop).

6.1 A small case study

In this section, we first introduce the small-scale example and test the applicability of our decomposition approach. Then, we illustrate how to manage the rescheduling problem with a seat reservation system. Finally, we investigate the influence of parameter ω.

6.1.1 Optimality test

To validate our integrated train rescheduling and passenger routing model, we first tested it on a small hypothetical railway network, as shown in Figure 7. This railway network consisted of seven stations from station S_1 to station S_7. Each station had two tracks, and each station track was adjacent to the platform, which meant that it could be used by trains to either dwell or pass. To simplify the model, we assumed that each side of the platform in a station served one station track. All the station tracks were numbered from 1 to 14. To carefully capture the running process of trains

and traveling process of passengers, the railway network was denoted by 42 points (i.e., the black spots). Three trains ran on the railway network: trains G_1 and G_2 ran from station S_1 to station S_6 without using station S_7, and train G_3 ran from station S_1 to station S_6 using station S_7 (see the dotted arrow lines shown in the figure). A disruption was modeled to occur in the segment between stations S_3 and S_4, and to block the segment for 25 mins from time 15-40 min. The planning horizon that we considered was from 1-90 min. The original timetable for these three trains is given in Table 5, together with both the arrival and departure times for each train at each station.

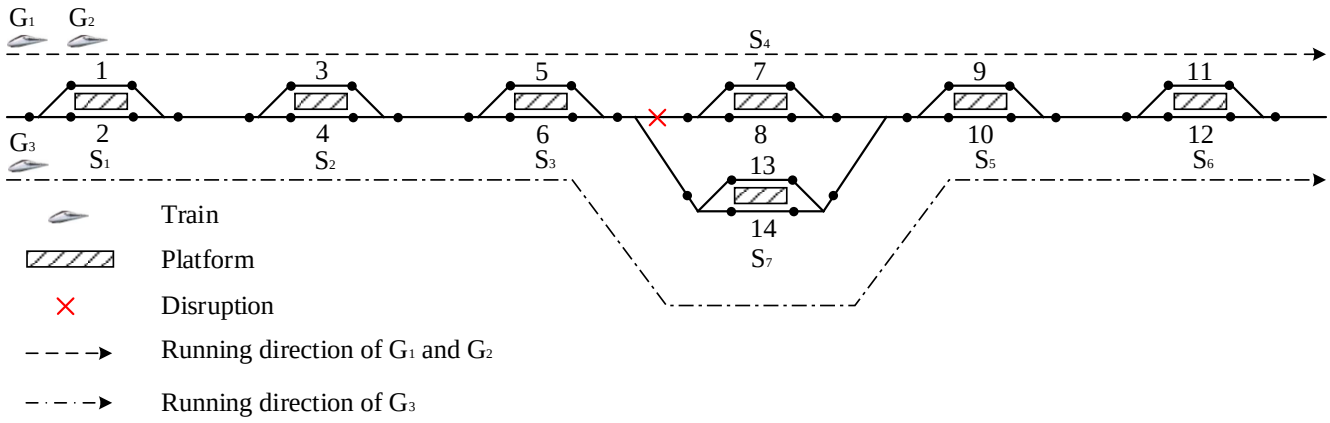

Figure 7: A small hypothetical railway network

Table 5: The original train timetable

Train	S_1	S_2	S_3	S_4	S_7	S_5	S_6
G_1	2-5	10-13	18-21	26-29	-	34-37	42-45
G_2	7-10	15-18	23-26	31-34	-	39-42	47-50
G_3	12-15	20-23	28-31	-	36-39	44-47	52-55

We assumed that all three trains ran at the same speed (five min per segment), and had the same scheduled dwell time in each station (three min). Each train served three passenger groups, as shown in Table 6, and each train could accommodate 30 passengers (q_k). The minimum headway of two trains running in a segment was three min, and the minimum headway for two trains using the same station track was zero min. However, as no train could pass the disrupted segment before the blockage was cleared, the earliest possible departure time of trains G_1 and G_2 from station S_3 was 41 min, one minute after the end of the disruption. As no anticipation of the occurrence of the disruption was allowed, trains were set to run as scheduled and use the same track as planned before the disruption occurred. Without loss of generality, we assumed that train G_1 used track 1 in station S_1 and track 3 in station S_2, train G_2 traveled on track 2 in station S_1 and track 4 in station S_2, and train G_3 utilized track 1 in station S_1. We set ω to one to give the same emphasis to both the train operation cost and passenger travel cost. If a train was canceled, the train operation cost is zero. If a passenger was rejected by all the trains, the penalty was 200. The time taken for a train stopped at a station track at its origin station or at a station track in its last station was three minutes. Therefore, trains arrived at their first station from the shunting yard three min before they departed from the first station, and trains left their last station to travel to the shunting yard three min after they arrived at their last station. The weight for each type of train arc and passenger arc is given in Table 7.

Using the values of parameters given above, we solved our integrated model by CPLEX. We obtained the optimal solution with an objective value of 7976 in nine seconds but with a relatively long preprocessing time to generate the model. This solution is the best to minimize both the train operation cost and the passenger travel cost. The detailed disposition timetable is in Table 8, and passenger route choice is shown in Table 9. In Table 9, for each passenger OD

Table 6: Passenger groups of each train

Passenger groups	Origin	Destination	Start time (min)	End time (min)	Volume	Planned train
1	29	42	11	90	10	G_3
2	29	41	11	90	10	G_3
3	29	38	11	90	10	G_3
4	29	42	1	90	10	G_1
5	29	41	1	90	10	G_1
6	29	38	1	90	5	G_1
7	29	42	6	90	10	G_2
8	29	41	6	90	5	G_2
9	29	38	6	90	5	G_2

Table 7: Values of weighted factors in the passengers' generalized travel time and train operation cost

Parameter	Description	Value	Unit
β_1	The weight for extra waiting time of passengers	2	[min/min]
β_2	The weight for transfer cost of passengers	10	[min/transfer]
β_3	The weight for late departure of passengers	1	[min/min]
α_2	The weight for extra stopping of trains	2	[min/min]
c	The train arc cost coefficient	2	[/min]

pair in each segment, we can see which train he/she took and how many passengers of this OD used the train. For example, 10 in the second row and second column indicates that 10 passengers in passenger group 1 took train G_3 in segment (S_1, S_2). The data in Table 9 also indicates that, passengers selected the shortest path with the lower general cost. For example, passenger group 6 transferred from train G_1 to train G_2 at station S_2 because train G_2 arrived at station S_3 earlier. Crucially, the train capacity constraint was always respected. It can be seen that the total number of passengers on train G_3 after the disruption was 30, which was equal to the train capacity, and the total number of passengers on train G_1 was 25, while the train capacity was 30.

Table 8: The disposition timetable obtained by CPLEX

Train	S_1	S_2	S_3	S_4	S_7	S_5	S_6
G_1	2-5	10-29	34-41	46-49	-	54-57	62-65
G_2	7-10	15-18	23-44	49-52	-	57-60	65-68
G_3	12-15	20-23	28-31	-	36-39	44-47	52-55

We also tested our decomposition approach using the same case. The initial values of Lagrangian multipliers ξ and γ were both set to 0.001, and the quadratic penalty parameters ρ_1 and ρ_2 were 4 and 0.7 respectively. Parameters up_1 and lo_1 were set to $0.3\rho_1$ and $-0.3\rho_1$, and up_2 and lo_2 were set to $0.6\rho_1$ and $-0.6\rho_1$. The outer layer iteration of train rescheduling and passenger routing was limited to ten, and the inner layer iteration of both train rescheduling and passenger routing were limited to five.

The best feasible solution within 10 outer iterations was obtained, and the current best objective value was 8036, which was the solution of iteration 3. The disposition timetable obtained by our decomposition approach is shown in Table 10. We compared the solution obtained by our decomposition approach with that obtained by CPLEX, and the optimality gap was 0.75%. The gap between the optimal solution and upper bound obtained by our decomposition approach is shown in Figure 8. It converged rapidly because the network is not very complicated. This optimality gap was good enough for real-world application. The passenger routing results are shown in Table 11. Passengers on train G_1 transferred to trains G_3 and G_2, which was different from the results in Table 9. This was because in our decomposition approach, train G_2 departed earlier than train G_1 after the disruption in the timetable, which was

Table 9: The passenger route choice obtained by solving the integrated model by CPLEX

OD	$S_1 - S_2$	$S_2 - S_3$	$S_3 - S_4$	$S_3 - S_7$	$S_4 - S_5$	$S_7 - S_5$	$S_5 - S_6$
1	G_3, 10	G_3, 10	-	G_3, 10	-	G_3, 10	G_3, 10
2	G_3, 10	G_3, 10	-	G_3, 10	-	G_3, 10	-
3	G_3, 10	G_3, 10	-	-	-	-	-
4	G_1, 10	G_1, 10	G_1, 10	-	G_1, 10	-	G_1, 10
5	G_1, 10	G_1, 10	G_1, 10	-	G_1, 10	-	-
6	G_1, 5	G_2, 5	-	-	-	-	-
7	G_2, 10	G_2, 10	-	G_3, 10	-	G_3, 10	G_3, 10
8	G_2, 5	G_2, 5	G_1, 5	-	G_1, 5	-	-
9	G_2, 5	G_2, 5	-	-	-	-	-

different from the departure time for these trains in the timetable obtained by CPLEX.

Table 10: The disposition timetable obtained by solving the integrated model by our decomposition approach

Train	S_1	S_2	S_3	S_4	S_7	S_5	S_6
G_1	2-5	10-13	18-44	49-52	-	57-60	65-68
G_2	7-10	15-26	31-41	46-49	-	54-57	62-65
G_3	12-15	20-23	28-31	-	36-39	44-47	52-55

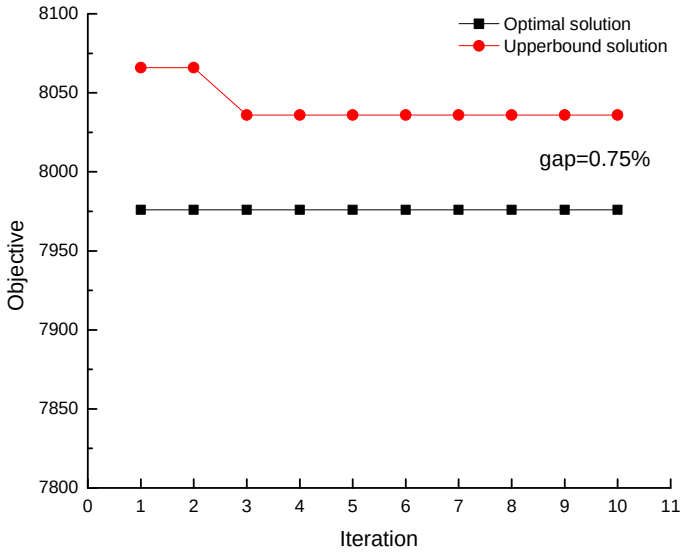

Figure 8: Optimality gap between the upper bound and the optimal solution

6.1.2 Seat reservation investigation

In the analysis in the previous subsection, we allowed passengers to freely choose their routes based on the general travel cost after a disruption occurred. Although the total passenger travel cost can be minimized in this manner, it is not a suitable solution for a railway network with a seat reservation system. For example, in Chinese high-speed railway, the seat reservation system does not allow passengers to freely select their routes like in the railway system which does not have a seat reservation system. This means that passengers who have already booked tickets for a train have priority to board their respective trains. Thus, given the limited capacity of a train, if a passenger wants to transfer from his/her reserved train to another earlier train, he/she must establish that a vacant seat is available in this earlier train. In addition, passengers normally do not like to have a temporary transfer during their journey because

Table 11: Passenger route choice obtained by solving the integrated model by our decomposition approach

OD	$S_1 - S_2$	$S_2 - S_3$	$S_3 - S_4$	$S_3 - S_7$	$S_4 - S_5$	$S_7 - S_5$	$S_5 - S_6$
1	G_3, 10	G_3, 10	-	G_3, 10	-	G_3, 10	G_3, 10
2	G_3, 10	G_3, 10	-	G_3, 10	-	G_3, 10	-
3	G_3, 10	G_3, 10	-	-	-	-	-
4	G_1, 10	G_1, 10	-	G_3, 10	-	G_3, 10	G_3, 10
5	G_1, 10	G_1, 10	G_2, 10	-	G_2, 10	-	-
6	G_1, 5	G_1, 5	-	-	-	-	-
7	G_2, 10	G_2, 10	G_2, 10	-	G_2, 10	-	G_2, 10
8	G_2, 5	G_2, 5	G_2, 5	-	G_2, 5	-	-
9	G_2, 5	G_2, 5	-	-	-	-	-

they know they must change their tickets before they are allowed to board another train. Therefore, the passenger allocation system in a disrupted situation on a railway network with seat reservation must be examined carefully. Based on current practice, we adopted the following strategies (below) for passenger allocation. Note that one can also use other rules to allocate passengers, e.g., give priority to important passengers.

- Passengers tend to travel on the trains they have booked a seat on if the booked trains continue operation. Thus, we gave priority to passengers to board their booked trains by setting a much lower cost for them to travel by booked trains.

- To prevent passengers temporarily transferring from their booked trains to other trains, we assigned a relatively high penalty cost for such a transfer.

- It was reasonable to allocate passengers who have booked the earlier trains first, as given the limited train capacity, passengers were not willing to transfer to later trains if their booked earlier trains were available.

Based on the given railway network, trains, and passenger groups in Section 6.1.1, we reduced the coefficient δ ($0 < \delta < 1$) of the cost that a passenger uses his/her reserved train. Therefore, if a passenger used the reserved train, the cost equaled the general cost multiple δ. In addition, we changed the transfer cost for passengers who have a temporary transfer during their journey because of the disruption. The value of coefficient δ and the transfer cost reflected how much freedom that the railway company allowed passengers to temporarily change trains.

We first tested the influence of different transfer penalty costs. We increased the penalty transfer cost from 10 to 60 with an interval of 10, and the value of all other parameters were unchanged. The test results are shown in Table 12. last column shows which passenger group had a temporary transfer. We can see that the objective value became larger with the increasing of transfer penalty cost. In addition, the number of transfers for passenger groups was reduced from three to zero when the transfer penalty cost increased from 10 to 60. Therefore, passengers tended to take their scheduled train, rather than trying to change trains, if the transfer cost increased. We can conclude that increasing the transfer penalty cost can prevent passengers freely transferring from their reserved train to other trains. We have not tested the influence of parameter δ here because the network was too small, and the influence of δ is not specially strong. We will investigate this further in the large case study.

6.1.3 Test of the influence of parameter ω

In this study, we minimized both the passenger travel cost and the train operation cost. We combined these two parts in the objective function containing parameter ω. It was found that the value of parameter ω could affect the results. If the value was small, this meant that we focused more on passenger travel cost; if the value was high, this meant that we focused on the train operation cost. To investigate this influence, we tested various values of parameter ω

Table 12: The sensitivity analysis of passenger transfer cost

Test	Transfer cost	Objective value	Number of transfers	Transfer passenger group
1	10	7976	3	6, 7, 8
2	20	8156	2	6, 7
3	30	8296	1	4
4	40	8396	1	4
5	50	8496	1	5
6	60	8496	0	-

in the simple case. The value of parameter ω varied from 1 to 50 with an interval of 10. The values of all other parameters were kept unchanged. However, we did not fix the schedule of trains and passengers before the occurrence of the disruption, as we wanted to see the influence of canceling trains. The results of this test are shown in Table 13. The last column of the table indicates the total number of canceled trains. The change of train operation cost and passenger travel cost with various values of ω is illustrated in Figure 9.

Table 13: The sensitivity analysis of parameter ω

Test	Value of ω	Objective value	Train operation cost	Passenger travel cost	Canceled train
1	1	7976	416	7560	0
2	10	11360	236	9000	1
3	20	12760	88	11000	2
4	30	13640	88	11000	2
5	40	14520	88	11000	2
6	50	15000	0	15000	3

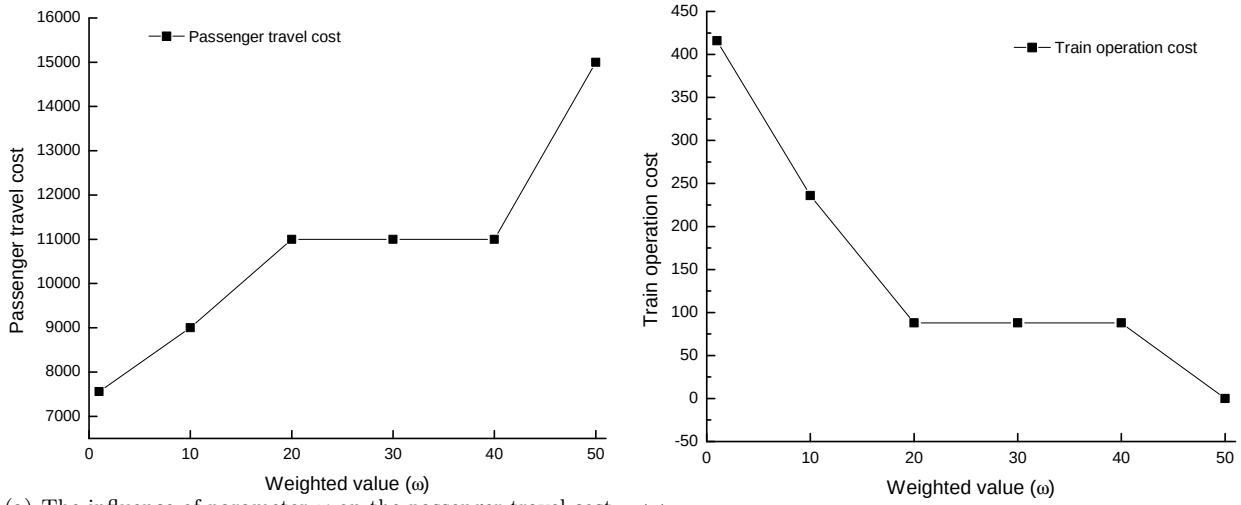

(a) The influence of parameter ω on the passenger travel cost

(b) The influence of parameter ω on the train operation cost

Figure 9: The influence of parameter ω on both the train operation cost and passenger travel cost

From Table 13 and Figure 9, we can see that when the value of parameter ω was small, i.e., $\omega = 1$, the train operation cost is 416, which is relatively high. Also, no train was canceled, but the passenger travel cost was low. With the increase of ω, the train operation cost reduces, while the passenger travel cost increases. In addition, more trains tended to be canceled when we increased the value of ω. When the value of ω was greater than 50, all three trains were canceled and the train operation cost is zero, but the passenger travel cost was quite high. This was because when all the trains were canceled, passengers could not be carried by any train and thus must give up traveling by train. Therefore, we showed that there is a trade-off between the train operation cost and passenger travel cost. Railway

managers can choose an appropriate value for parameter ω, based on their experience to achieve a balance between these opposing factors.

6.2 A large case study

6.2.1 Test instances and parameter values

To validate our model and solution approach, we tested them on part of a real-world high-speed railway network in China. This railway network consisted of three high-speed railway lines. One was the Jinan-Nanjing high-speed railway line, which is the middle part of the Beijing-Shanghai high-speed railway line (see the red line in Figure 10). Another was the Hefei-Bengbu intercity high-speed railway line (see the yellow line in Figure 10). The third was the Nanjing-Hefei high-speed railway line, which is the middle part of the Shanghai-Chengdu high-speed railway line (see the blue line in Figure 10). For more information about the Chinese high-speed railway network, we refer the readers to Zhan et al (2016). Our study railway network consisted of 17 stations, which are denoted by circles. Large stations that could be used for a trains original departure and final arrival are denoted by double circles in the figure, while relatively small stations are denoted by single circles. As the tracks in large stations are used separately by trains from different lines, we divided Hefei South Station and Nanjing South Station into two stations, which are connected by black lines in the figure. The number of station tracks is shown beside each station as a number in a bracket. It can be seen that some stations are very large, i.e., Nanjing South Station has 22 tracks. Although we considered the train routing in a station area at a microscopic level, it is difficult to show the layout of all the stations, and thus we only show that of a relatively small station, the Chuzhou Station, as an example in Figure 10.

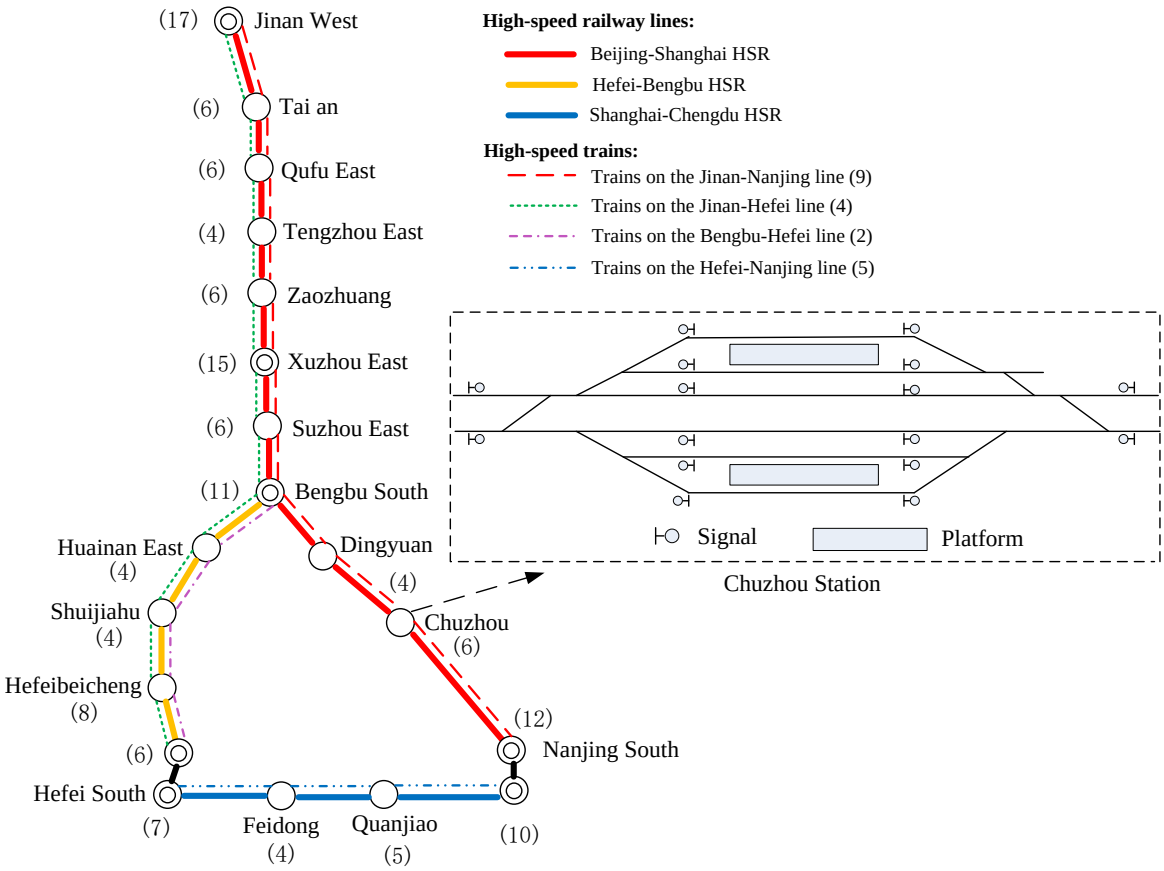

Figure 10: A part of the Chinese high-speed railway network

We assumed that a disruption occurred in the segment between Bengbu South Station and Dingyuan Station of

the Jinan-Nanjing high-speed railway line at 12:00. It lasted to 14:00, and both tracks of the disrupted segment are unavailable during the disrupted period.

In practice, railway managers tend to prevent the influence of a disruption on one line propagating to other non-disrupted lines. Train rerouting is not allowed, as previously mentioned. Therefore, it is reasonable to assume that during a disruption, trains that run on the Nanjing-Hefei high-speed railway line continue to use the same track as scheduled, but their departure and arrival time may be slightly modified to smooth the transfer of passengers from the disrupted line. Similarly, trains that only run on the Hefei-Bengbu inter-city high-speed railway line may have their departure and arrival times modified, too. This assumption is also helpful to reduce the burden of searching for train and passenger routes. However, trains that run on the Jinan-Nanjing high-speed railway line and trains that partly run on this line and then run on the Hefei-Bengbu inter-city line should all be completely rescheduled, as they are affected by the disruption. Passengers on these trains can reroute to use trains on the other two lines, if necessary. Our problem is a real-time problem and the exact duration of the disruption is usually unknown in advance, which means it is not necessary to reschedule all trains and passengers for a whole day. Instead, we considered a planning horizon of 6 hours (i.e., the horizon of the space-time network is 6 hours), from 10:00 to 16:00, which is the busiest period. During this period, we studied trains and passengers that departed from their origins within 2 hours. However, the running processes of these trains and the travel processes of these passengers within the 6-hour planning horizon are considered because a train takes approximately 3 hours to travel from Jinan West Station to Nanjing South Station; see, for example, Figure 13. Trains and passengers in other periods could be iteratively rescheduled in the same way by a rolling horizon approach (Zhan et al (2016)).

According to the timetable used in the last six months of 2015 (normally the timetable is updated in the middle of each year for Chinese railway), there were nine trains running from Jinan West Station to Nanjing South Station, four trains running from Jinan West Station to Hefei South Station, two trains running from Bengbu South Station to Hefei South Station, and five trains running from Hefei South Station to Nanjing South Station. The routes for these trains and the flow of trains on each route are shown in Figure 10 by various lines and by the number in brackets after the line. Note that we only considered high-speed trains with a speed of 300 km/h or 350 km/h, which are called "G" trains; high-speed trains with a lower speed of 200 km/h or 250 km/h, called "D" trains, were not considered in this case study. Therefore, there were 20 trains in total operated on the study railway network in one direction during two hours. The minimum dwell time of each train in each station was set to two min, and the running time of each segment is shown in Table 14. The capacity of a high-speed train is 1000 passengers, according to current practice. We rescheduled trains for one direction, and thus we assumed that half of the tracks in each station could be used by these trains. The train rescheduling in the other direction was similar. The minimum headway (h_{dep}^{min} and h_{arr}^{min}) in a segment was three min, and the minimum station headway ($h_{station}^{min}$) was zero min.

Table 14: The running time in each segment between two stations

No.	Segment	Time (min)	No.	Segment	Time (min)
1	Jinan West - Tai'an	12	10	Chuzhou - Nanjing South	16
2	Tai'an - Qufu East	15	11	Bengbu South - Huainan East	13
3	Qufu East - Tengzhou East	11	12	Huainan East - Shuijiahu	6
4	Tengzhou - Zaozhuang	7	13	Shuijiahu - Hefeibeicheng	10
5	Zaozhuang - Xuzhou East	13	14	Hefeibeicheng - Hefei South	24
6	Xuzhou East - Suzhou East	14	15	Hefei South - Feidong	9
7	Suzhou East - Bengbu South	18	16	Feidong - Quanjiao	25
8	Bengbu South - Dingyuan	11	17	Quanjiao - Nanjing South	20
9	Dingyuan - Chuzhou	13			

The passenger information of the Jinan-Nanjing high-speed railway line was based on real data from the ticket

booking system, but we have revised some of this because we only considered part of the data, and the real passenger data is confidential. The passenger OD for another two lines were revised as we only considered a part of the line. When we generated the OD matrix, the loading rate of each train was maintained at approximately 70%. In total, we generated 89 passenger groups, of which 50 were on the Jinan-Nanjing line, 28 were on the trains from Jinan West to Hefei South, six booked the tickets for trains on the Bengbu-Hefei inter-city line, and five passenger groups booked the tickets for trains on the Hefei-Nanjing line. As the Hefei-Nanjing high-speed railway line was a short part of the Shanghai-Chengdu high-speed railway line, and the exact passenger data was not available at this time, we generated one OD pair for each train from Hefei South Station to Nanjing South Station, for simplicity. As mentioned previously, passengers on this line were not significantly affected by the disruption and stayed on their booked train. Thus, the exact OD matrix for these passengers is not required, as passengers on the disrupted line were our main focus.

6.2.2 Computational results

6.2.2.1 Test of our decomposition approach Based on the provided train and passenger information, and the assumed disruption scenario, we tested our decomposition approach. The initial values of Lagrangian multipliers ξ and γ were both set to 0.001. The quadratic penalty parameters ρ_1 and ρ_2 were 40 and 0.2 respectively, which were analyzed in Appendix B. Parameters up_1 and lo_1 were set to $0.3\rho_1$ and $-0.3\rho_1$, and up_2 and lo_2 were set to $0.6\rho_1$ and $-0.6\rho_1$. The value of ω was 1. The values of weighted factors for passengers' travel cost and train operation costs are shown in Table 17. The outer iteration was limited to twenty steps, while the inner iteration for train rescheduling was set to five and for passenger routing was set to two.

Table 15: The values of weighted factors in the passengers' generalized travel time and train operation cost

Parameter	Description	Value	Unit
β_1	The weight for extra waiting time of passengers	2	[min/min]
β_2	The weight for transfer cost of passengers	10	[min/transfer]
β_3	The weight for late departure of passengers	3	[min/min]
α_1	The weight for late departure of trains	2	[min/min]
α_2	The weight for extra stopping of trains	2	[min/min]
c	The train arc cost coefficient	1	[/min]

The current solution and the best upper bound solution for each iteration are shown in Figure 11. The current solution for each iteration fluctuates, and the current solutions are infeasible for some iterations, as denoted by green dotted circles in the Figure. The obtained solutions for seven iterations are infeasible, which results in an infeasibility rate of 35% in this case study. This infeasibility is caused by the infeasible disposition timetable obtained within five inner iterations for each outer iteration step. From Figure 11, we can see that the best upper bound solution decreases significantly until iteration 7, and then it is quite stable until iteration 20. Therefore, the solution obtained in the 7th iteration can be regarded as a good one for practical application, considering that our problem is a real-time problem. The computation time for seven outer iterations (each outer iteration includes five iterations for train rescheduling and two iterations for passenger routing) is around 23 min, and about 3 min is required for each outer iteration calculated on a personal computer. The objective of the solution obtained at iteration 7 was 1,658,506 (train operation cost 3,598 and passenger travel cost 1,654,908), which was *7%* less than that of the solution obtained at iteration 1. According to our test, this decrease occurs mainly because a better disposition timetable for trains is obtained and the passengers can find better paths in iteration 7 (i.e., the coordination between train rescheduling and passenger routing is better in the upper bound solution of iteration 7). Five passenger groups (from Jinan West to Nanjing South) have transfers from the Jinan-Nanjing line to the Bengbu-Hefei line and then to Hefei-Nanjing line to arrive at their destination in the upper bound solution of iteration 7. However, only three passenger groups that depart from Jinan West have the

same transfers to Nanjing South, and non-transfer passengers must wait a long time during the disruption, in the upper bound solution of iteration 1.

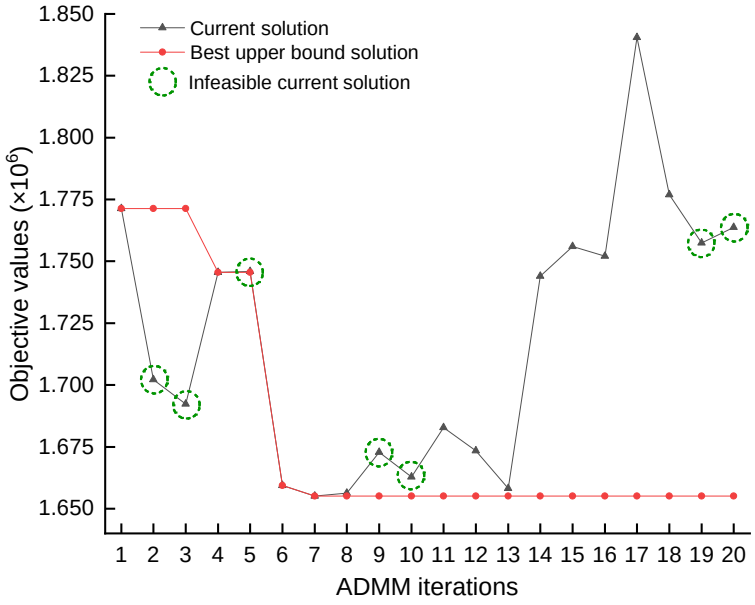

Figure 11: Upper bound solution for each iteration

To evaluate the quality of the best upper bound solution obtained above by ADMM in the seventh iteration, we compute the lower bound of the same case with LR. The maximum iteration step between the train rescheduling and passenger routing problems is set to 100, and for the train rescheduling in each outer step, we update the train rescheduling subproblem for 50 iterations (i.e., the maximum inner LR iteration step is set to 50) to obtain a relatively good disposition timetable. The value of parameter ϵ is set to 0.05. Figure 12 illustrates the lower bound solutions for 100 iteration steps. The best lower bound obtained within 100 iterations is 1,442,901, and the optimality gap between the best upper bound solution obtained with ADMM in iteration 7 and the best lower bound solution obtained by LR within 100 iterations is *14.9%*.

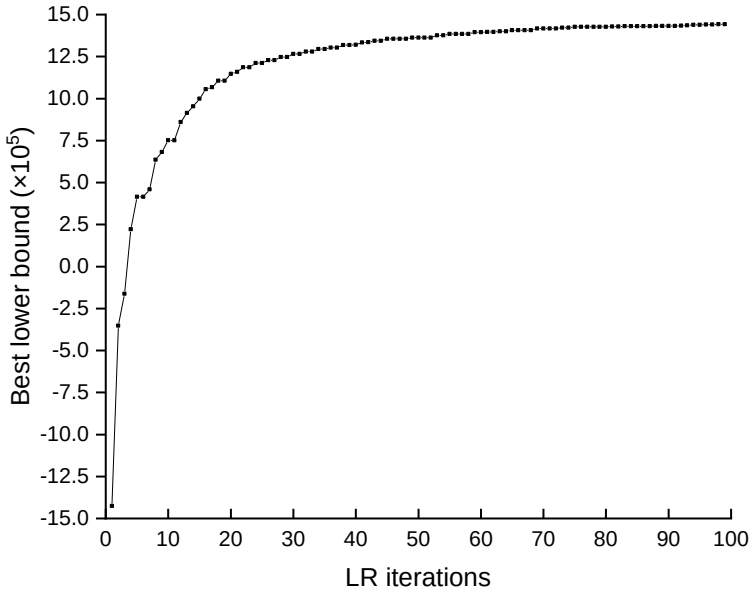

Figure 12: Lower bound solution for each outer iteration obtained with LR

We obtained a good feasible solution (with an optimality gap of 14.9%) for all the 20 trains of the considered railway

network, and we showed the disposition timetable for the Jinan-Nanjing high-speed railway line as an example (see in Figure 13). We numbered the nine trains according to their departure order, and this number is beside the line of each train in the figure. We can see that disrupted trains wait at appropriate stations for the disruption. No conflict existed between any two trains, and the station capacity constraint was respected in each station.

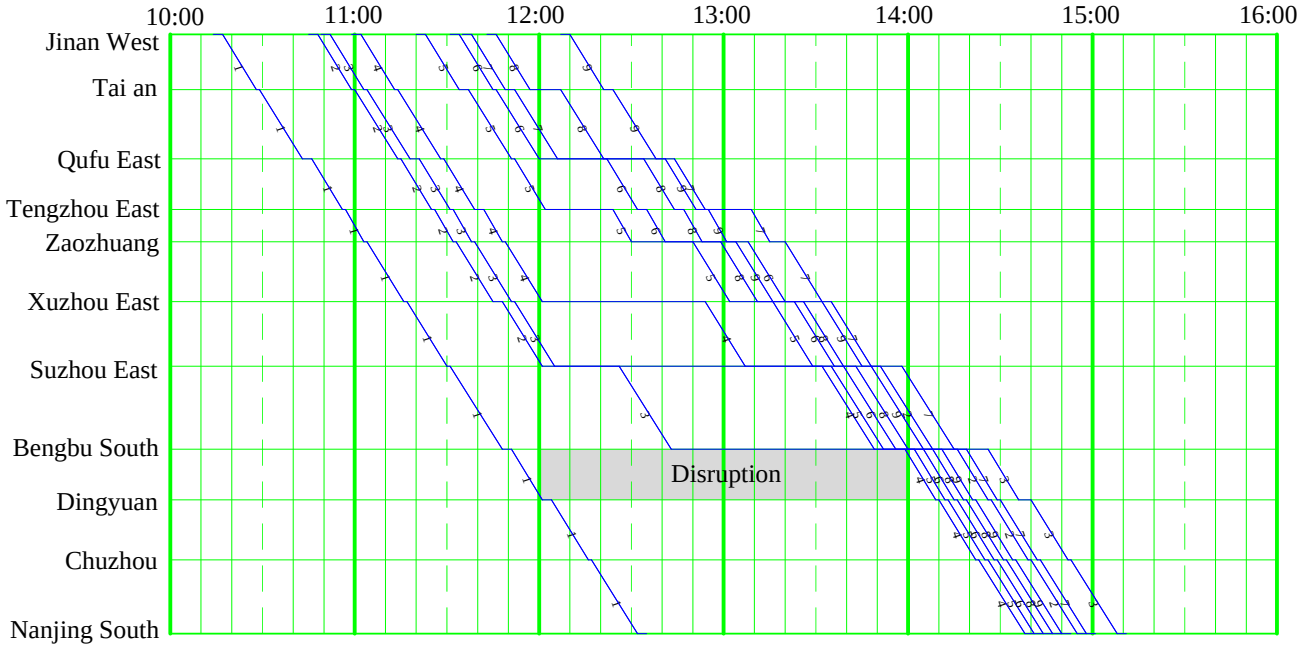

Figure 13: A disposition timetable for the Jinan-Nanjing high-speed railway line

As no train was canceled in this case, most passengers took their booked trains to their destination. In total, five passenger groups that planned to travel on the Jinan-Nanjing high-speed line to Nanjing South Station transferred due to the disruption to trains that ran on the Bengbu-Hefei and Hefei-Nanjing high-speed lines to their destination. This rerouting helped to reduce their total travel cost and they arrived at their destination earlier.

6.2.2.2 Analysis of the parameter for ticket reservation

Because the seat reservation system is applied in Chinese high-speed railway, passengers may not decide to transfer from their reserved train to other trains if they cannot save significant travel costs. We earlier outlined two strategies to manage passengers transfer in a seat reservation system. The first strategy was to improve the transfer cost to reduce the probability of transfer (see the analysis in Section 6.1.2). The second strategy was to set a parameter δ to manage passengers' transfer preference. That is, we reduced the cost of the path used by passengers, to attract passengers to their reserved trains when their reserved trains are not canceled due to the disruption in passenger routing process. To illustrate the influence of parameter δ on passengers' route choice, we ran our example several times with various parameter values. The values were set from 1 to 0.4 with a decrease interval of 0.2. The results are shown in Table 16. The fourth column is the total number of passenger groups that transferred to use trains on other lines, and the last column shows which passenger group was rerouted.

Table 16: The sensitivity analysis of parameter δ

Test	Value of δ	Objective of best solution	Number of rerouting	Rerouting passenger groups
1	1	1655213	5	50, 51, 54, 57, 58
2	0.8	1730818	3	50, 51, 58
3	0.6	1744740	1	58
4	0.4	1820366	1	58

From Table 16, we can see that reducing the value of parameter δ can prevent passengers transferring and rerouting during their journey. Specifically, when the value of δ is one, five passenger groups performed a temporary rerouting during their journey due to the disruption. Specifically, they rerouted to use trains on the Bengbu-Hefei and Hefei-Nanjing high-speed railway lines to continue their journey instead of waiting for their planned trains that were disrupted on the Jinan-Nanjing high-speed railway line. Here $\delta = 1$ meant that we did not reduce the cost of arcs on the passenger reserved path. If we decreased the value of δ to 0.4, only one passenger group rerouted. It is possible that if we further reduced the value of δ, no passengers would reroute because no train in our case is canceled and passengers will keep on their reserved trains. Therefore, our finding suggests that railway managers can select value of parameter δ to reduce the freedom of passengers' temporary transfer and reinforce the passengers' preference to stay on their reserved trains in a railway system with seat reservation. However, if more passengers remain on their reserved train without a transfer or rerouting, the total passenger travel cost is higher because the delay for some passengers is longer. This trend can also be seen in Table 16, as the increasing of the objective value in the third column.

6.2.2.3 Analysis of the trade-off between train operation cost and passenger travel cost

The trade-off between the train operation cost and passenger travel cost in the objective function of our integrated model has been analyzed for the small case study in Section 6.1.3. It showed that the passenger travel cost increased and the train operation cost decreased when parameter ω increases. We also test this trade-off for our large case study. However, we do not change the value of parameter ω to represent different weights for the two components in the objective function. Instead, we cancel different numbers of trains to reveal the trade-off between the train operation cost and passenger travel cost. Because our decomposition approach is a heuristic method and different values of parameter ω require different values of penalty parameter ρ_1 to ensure the feasibility of the obtained train disposition timetable, the obtained solutions with various values of ω are not comparable. As the train operation cost is mainly affected by the number of canceled trains, we use different numbers of canceled trains to illustrate the trade-off.

We cancel one to four trains in the input timetable, and thus a total of five tests, where the first test with no train cancelation is the solution obtained in Section 6.2.2. For each of the other four tests, we test three scenarios where the same number of different trains are chosen to be canceled, and then the average solution for each test is shown in Table 17. In this table, the fourth column ("TOC") is the train operation cost, and the fifth column ("PTC") is the passenger travel cost. The last column specifies which trains are canceled in the test. For tests two to four, each has three braces, which means that we choose three different combinations of trains to be canceled. Each number in a brace is a canceled train, and the number of each train on the Jinan-Nanjing high-speed railway line is shown in Figure 13. Except that train 10 is scheduled to run on the Jinan-Hefei high-speed railway line, all the other trains (from numbers 1 to 9) are operated on this line.

Table 17: The trade-off between the two components of the objective function

Test	Total cancelations	Objective	TOC	PTC	Canceled trains
1	0	1658506	3598	1654908	-
2	1	1714599	3281	1711318	{2}; {4}; {6}
3	2	1725272	2967	1722305	{2,4}; {3,5}; {4,6}
4	3	1805789	2713	1803076	{2,4,6}; {3,5,7}; {5,7,9}
5	4	1907682	2527	1905155	{2,4,6,8}; {3,5,7,9}; {4,6,8,10}

According to the solutions given in Table 17, the passenger travel cost and train operation cost for each test are illustrated in Figure 14. We can see that the train operation cost decreases and the passenger travel cost increases when more trains are canceled, i.e., a trade-off exists between the train operation cost and passenger travel cost. This

trend is consistent with that shown in Figure 9 in the small case study.

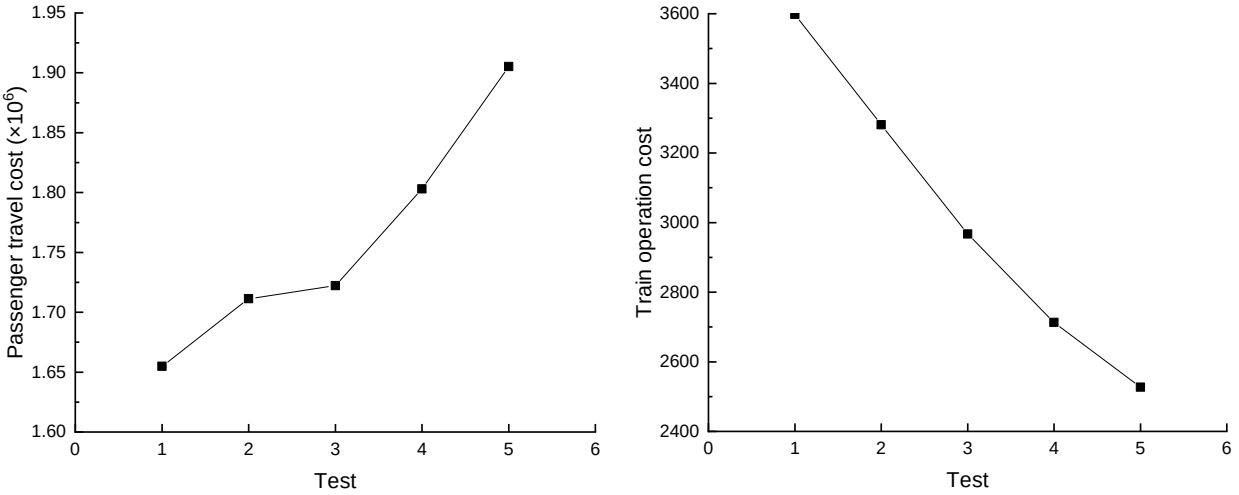

(a) The influence of train cancelation on the passenger travel cost

(b) The influence of train cancelation on the train operation cost

Figure 14: The influence of train cancelation on both the train operation cost and passenger travel cost

6.2.2.4 Computation efficiency analysis

The problem that we focused on is a complicated one, and even the train scheduling (rescheduling) problem is NP-hard in its own right. Thus, it is impossible to solve our integrated problem in a short computation time for a large real-world problem using a commercial solver, e.g., CPLEX. A similar problem for a part of Dutch railway network is solved in hours in Binder et al (2017b). In their case, the network consists of 11 stations (each station only has two tracks) and 24 trains operated in a time horizon of two h, and 50 passenger groups were considered. In addition, a time interval of five min was applied in their space-time network. Thus, they assumed that the headway between trains and the dwell time for a train in a station were both one time interval (five min), and the additional constraints for trains running in the same direction on a track did not need to be considered.

We mainly focused on high-speed railways, where a time interval of five min for the space-time network is not accurate enough. Therefore, we used one min as the time interval, and the constraints for headway and dwell time of trains needed to be carefully taken into account, which made the model harder to solve. In addition, we rescheduled trains and passengers with high detail, which significantly increased the number of variables and constraints. Finally, compared with the case in Binder et al (2017b), our case considered a larger network within a much longer time horizon, examined 17 stations with most stations having more than two tracks, and 91 passenger groups (almost double). Therefore, we imagine that our problem cannot be solved by CPLEX directly.

We compared the computation efficiency of our decomposition approach and CPLEX by simplified cases based on our large case. We selected two trains on the Jinan-Nanjing high-speed railway line and 11 passenger groups corresponding to these two trains. We ran an analysis of this simplified case by CPLEX for a long time, but we could not obtain a feasible solution within 24 h. This demonstrated that our decomposition approach is quite efficient in solving our integrated problem, especially as we can get a good feasible solution for a large case in minutes.

6.2.2.5 Comparison with no passenger rerouting

To investigate whether our integrated train rescheduling and passenger routing approach outperforms train rescheduling without passenger rerouting (i.e., rescheduling trains only and keeping passengers on their reserved trains), we solve our large case by only rescheduling trains for comparison. Similar to the approach used by Zhan et al (2015) that only reschedules trains, we first reschedule trains to obtain a near-optimal disposition timetable. Based on the obtained

train timetable, we calculate the travel cost for passengers who remain on their reserved trains. That is, rerouting passengers is not allowed if their reserved trains are in operation. We use the model **Px** in Section 5.1 to model the pure train rescheduling problem, and the relaxation of coupling constraint (14) in **Px** is no longer necessary. Therefore, this pure train rescheduling problem can be solved by ADMM in the same way as explained in Section 5.2. After we have obtained a good feasible disposition timetable, we can calculate the total passenger travel cost. To calculate the total passenger travel cost, we can use a similar method to generate the upper bound (i.e., Algorithm E in the Appendix). However, because it is unnecessary to reroute passengers because no trains are canceled in this case, we do not allow transfers, and passengers are only allowed to use their reserved trains in Algorithm E.

If all parameters maintain the same values as before, we obtain a feasible solution with an objective value of 1,734,847, where the total passenger cost is 1,731,403 and the total train operation cost is 3,444. Compared with the best upper bound solution obtained at iteration 7 in Section 6.2.2.1, the total passenger travel and train operation cost increases by 4.6%. Accordingly, the integrated train rescheduling and passenger routing approach is better to reduce the passenger travel cost.

7 Conclusion

Real-time train rescheduling during a complete track blockage is important for train dispatchers and passengers. In this research, we have extended the train rescheduling problem in Zhan et al (2015) to include passenger route choice. The integrated train rescheduling and passenger routing is formulated by an ILP model based on a space-time network. In our model, the detailed feasible train disposition timetable as well as the specific routes for each train was obtained. In addition, the routes for passengers were optimized considering the limited train capacity in a disruption. The model was found to be suitable for railway systems without seat reservations assuming that the passenger OD demands are known before and after the disruption occurs (Binder et al (2017b)). However, we have introduced several strategies to manage train rescheduling and passenger routing problem with seat reservation because this is usually used on Chinese high-speed railway system.

In recognition of the complexity of the integrated problem, we introduced a two-layer dual decomposition approach to decompose the whole problem into several easy-to-solve subproblems. Specifically, we relaxed the coupling constraint and decomposed the integrated problem into two subproblems, a train rescheduling subproblem and a passenger routing subproblem, using ADMM in the first layer. As the headway and station capacity constraints are related to many trains instead of each single train, we relaxed these two constraints to decompose the train rescheduling subproblem in the second layer by ADMM into many single-train rescheduling subproblems, and each one could be regarded as a shortest path searching problem. Similarly, the passenger routing subproblem could be decomposed into many smaller subproblems (shortest path searching), one for each passenger group. The shortest path searching subproblem either for each train or each passenger group was solved by a dynamic programming algorithm.

We have tested our model on a small railway network to illustrate that rescheduling trains and passengers simultaneously can generate a better disposition timetable from passengers perspectives. In addition, our approach could guide the disrupted passengers to select a better route to their destination. In the simple case, the objective value obtained by our decomposition approach was 0.75% larger than that obtained by CPLEX (the optimal solution) within five iterations. Therefore, our algorithm was useful for accessing a good, feasible solution.

We also found that there is a trade-off between minimizing train operation cost and minimizing passenger travel cost. Railway managers can put various emphases on the two objectives, according to their preference, to obtain a train disposition timetable and passenger routing plan. In our large case study, the problem cannot be solved by CPLEX in days. However, our approach makes it solvable in minutes. Our decomposition approach yielded a feasible

solution after seven iterations, which will be helpful for railway dispatchers. Specifically, the objective value of the feasible solution obtained by our decomposition approach at iteration 7 was 7% smaller than that obtained in the first iteration. The optimality gap between the best feasible solution and the best lower bound solution obtained by LR was 14.9%.

We have introduced a two-layer decomposition approach by using ADMM to solve our integrated problem. Some important parameters were analyzed by sensitivity tests. However, a theoretical analysis of these parameters is necessary in future research. In addition, our decomposition approach is heuristic, and an exact approach is desirable to obtain the optimal solution to theoretically evaluate the quality of the decomposition approach. Besides, the rescheduling of rolling-stock is not considered in this research, and may need to be taken into account in future work. Finally, because a trade-off exists between the short-turning strategy and the waiting strategy, a detailed comparison of these two strategies in a major disruption would be of interest.

Acknowledgments

The work described in this paper was supported by a grant from the Research Grants Council of the Hong Kong Special Administrative Region, China (Project No. [T32-101/15-R]), the National Natural Science Foundation of China (NSFC) (No.71701174 and No.61603317), the National Key R & D Plan of China (No. 2017YFB1200701) and the Fundamental Research Funds for the Central Universities (No.2682017CX020). The first author was supported by the Hong Kong Scholar Scheme 2017. The second author was supported by the Francis S Y Bong Endowed Professorship in Engineering.

Appendix A

A.1 The nonlinear term for the headway and station capacity constraint (9) in subproblem **Px:**.

Considering the quadratic term $\left(\sum_{k\in K}\sum_{a\prime\in\Phi(a)} x_{a\prime}^k - 1 + r_a\right)^2$ derived from constraint (9a), the purpose of introducing the slack variable r_a is to: (1) add a penalty term $\left(\sum_{k\in K}\sum_{a\prime\in\Phi(a)} x_{a\prime}^k - 1\right)^2$ in the objective function (Equation (18)) when constraint (9) is violated; (2) lead the penalty term $\left(\sum_{k\in K}\sum_{a\prime\in\Phi(a)} x_{a\prime}^k - 1\right)^2$ to 0 when constraint (9) is satisfied. Obviously, when $\sum_{k\in K}\sum_{a\prime\in\Phi(a)} x_{a\prime}^k > 1$, constraint (9) is violated. Therefore we can set $r_a = 0$ to transform the quadratic term $\left(\sum_{k\in K}\sum_{a\prime\in\Phi(a)} x_{a\prime}^k - 1 + r_a\right)^2$ into the quadratic penalty term $\left(\sum_{k\in K}\sum_{a\prime\in\Phi(a)} x_{a\prime}^k - 1\right)^2$; when $\sum_{k\in K}\sum_{a\prime\in\Phi(a)} x_{a\prime}^k \le 1$, constraint (9) is satisfied, therefore we can set $r_a = 1 - \sum_{k\in K}\sum_{a\prime\in\Phi(a)} x_{a\prime}^k$ to transform the quadratic term $\left(\sum_{k\in K}\sum_{a\prime\in\Phi(a)} x_{a\prime}^k - 1 + r_a\right)^2$ into zero. Thus, the value of r_a can be expressed by Equation (25).

$$r_a = \begin{cases} 0 & \sum_{k\in K}\sum_{a\prime\in\Phi(a)} x_{a\prime}^k > 1 \\ 1 - \sum_{k\in K}\sum_{a\prime\in\Phi(a)} x_{a\prime}^k & \sum_{k\in K}\sum_{a\prime\in\Phi(a)} x_{a\prime}^k \le 1 \end{cases} \tag{25}$$

To divide the quadratic term $\left(\sum_{k\in K}\sum_{a\prime\in\Phi(a)} x_{a\prime}^k - 1 + r_a\right)^2$ into several independent terms for each train k and solve the subproblem P_x^k sequentially, we need to separate out the variables related with train k from the other trains. To this end, we define $\psi_a^k = \sum_{k\prime\in K/k}\sum_{a\prime\in\Phi(a)} x_{a\prime}^{k\prime}$ to denote the total number of trains excluding k that use the arcs in $\Phi(a)$, and we have $x_a^k + \psi_a^k + r_a = 1$. According to the nature of ADMM, for each subproblem P_x^k, the term ψ_a^k is known, the value of r_a could be expressed as Equation (26).

$$r_a = \begin{cases} 0 & \psi_a^k \ge 1 \\ 1 - x_a^k & \psi_a^k = 0 \end{cases} \tag{26}$$

Then, we substitute the variable r_a in the quadratic term $\left(\sum_{k\in K}\sum_{a\prime\in\Phi(a)} x_{a\prime}^k - 1 + r_a\right)^2$ with r_a in Equation (26), we can get Equation (27) and Equation (28), where R denotes the summation of all the constant terms $(\psi_a^k - 1)^2$ in Equation (27).

$$\left(\sum_{k\in K}\sum_{a\prime\in\Phi(a)} x_{a\prime}^k - 1 + r_a\right)^2 = \begin{cases} \sum_{a\prime\in\Phi(a)} x_{a\prime}^k \times \left(2\psi_a^k - 1\right) + \left(\psi_a^k - 1\right)^2 & \psi_a^k \ge 1 \\ 0 & \psi_a^k = 0 \end{cases} \tag{27}$$

$$\left(\sum_{k\in K}\sum_{a\prime\in\Phi(a)} x_{a\prime}^k - 1 + r_a\right)^2 = \begin{cases} \sum_{a\prime\in\Phi(a)} x_{a\prime}^k \times \left(2\psi_a^k - 1\right) + R & \psi_a^k \ge 1 \\ 0 & \psi_a^k = 0 \end{cases} \tag{28}$$

In Equations (27) and (28), when $\psi_a^k \geq 1$, the detailed process is as follows (Equation (29)):

$$\begin{aligned}(\sum_{k\in K}\sum_{a'\in\Phi(a)} x_{a'}^k - 1 + r_a)^2 =&(\sum_{k\in K}\sum_{a'\in\Phi(a)} x_{a'}^k - 1)^2 = (\sum_{a'\in\Phi(a)} x_{a'}^k + \psi_a^k - 1)^2\\ =&(\sum_{a'\in\Phi(a)} x_{a'}^k)^2 + 2\times\sum_{a'\in\Phi(a)} x_{a'}^k\times(\psi_a^k-1) + (\psi_a^k-1)^2\\ =&(\sum_{a'\in\Phi(a)} x_{a'}^k + 2\times\sum_{a'\in\Phi(a)} x_{a'}^k\times(\psi_a^k-1) + (\psi_a^k-1)^2\\ =&(2\times\psi_a^k-1)\times\sum_{a'\in\Phi(a)} x_{a'}^k + (\psi_a^k-1)^2\\ =&(2\times\psi_{a'}^k-1)\times\sum_{a'\in\Phi(a)} x_{a'}^k + R\end{aligned} \tag{29}$$

A.2 The nonlinear term for the coupling constraint (14) in subproblem **Px:**.

The above process can be applied to linearize the quadratic term $\left(\sum_{p\in P} n_p\times\bar{v}_a^p - \sum_{k\in K} q_k\times x_a^k + s_a\right)^2$. Parameter μ_a^k denotes the capacity of trains excluding k that use arc a, $\mu_a^k = \sum_{k'\in K/k} q_{k'}\times x_a^{k'}$, and W denotes the summation of all the constant terms. When scheduling current train k, we compare the total number of passengers that have been assigned to an arc a, $\sum_{p\in P} n_p\times\bar{v}_a^p$, and the total number of available train capacity μ_a^k. If $\sum_{p\in P} n_p\times\bar{v}_a^p > \mu_a^k$, it means that the current capacity cannot meet the demand of passengers' requirement on arc a, so that we must attract train k to arc a. Thus, the quadratic term in objective (18) is not necessary. However, if $\sum_{p\in P} n_p\times\bar{v}_a^p \leq \mu_a^k$, it means that the current capacity of trains can already meet the passengers' requirement on arc a. Therefore, train k is not necessary to run on arc a, and the quadratic term in objective (18) is added to prevent train k using arc a. Accordingly, the value for slack variable s_a can be defined as follows (Equation (30)):

$$s_a = \begin{cases} 0 & \sum_{p\in P} n_p\times\bar{v}_a^p \leq \mu_a^k \\ q_k\times x_a^k + \mu_a^k - n_p\times\sum_{p\in P} n_p\times\bar{v}_a^p & \sum_{p\in P} n_p\times\bar{v}_a^p > \mu_a^k \end{cases} \tag{30}$$

Based on the value of variable s_a in Equation (30), the quadratic term in objective (18) is changed to Equation (31), where W is the constant term and $W = (\sum_{p\in P} n_p\times\bar{v}_a^p - \mu_a^k)^2$.

$$(\sum_{p\in P} n_p\times\bar{v}_a^p - \sum_{k\in K} q_k\times x_a^k + s_a)^2 = \begin{cases} q_k\times(q_k + 2\times\mu_a^k - 2\times\sum_{p\in P} n_p\times\bar{v}_a^p)\times x_a^k + W & \sum_{p\in P} n_p\times\bar{v}_a^p \leq \mu_a^k \\ 0 & \sum_{p\in P} n_p\times\bar{v}_a^p > \mu_a^k \end{cases} \tag{31}$$

When $\sum_{p\in P} n_p\times\bar{v}_a^p \leq \mu_a^k$, the detail process to obtain Equation (31) from (30) is as follows (Equation (32)):

$$\begin{aligned}(\sum_{p\in P} n_p\times\bar{v}_a^p - \sum_{k\in K} q_k\times x_a^k + s_a)^2 =&(\sum_{p\in P} n_p\times\bar{v}_a^p - \sum_{k\in K} q_k\times x_a^k)^2 = (\sum_{p\in P} n_p\times\bar{v}_a^p - (\mu_a^k + q_k\times x_a^k))^2\\ =&(\sum_{p\in P} n_p\times\bar{v}_a^p - \mu_a^k)^2 - 2\times(\sum_{p\in P} n_p\times\bar{v}_a^p - \mu_a^k)\times q_k\times x_a^k + (q_k\times x_a^k)^2\\ =&(\sum_{p\in P} n_p\times\bar{v}_a^p - \mu_a^k)^2 - 2\times(\sum_{p\in P} n_p\times\bar{v}_a^p - \mu_a^k)\times q_k\times x_a^k + (q_k)^2\times x_a^k\\ =&q_k\times(q_k + 2\times\mu_a^k - 2\times\sum_{p\in P} n_p\times\bar{v}_a^p)\times x_a^k + W\end{aligned} \tag{32}$$

A.3 The nonlinear term for the coupling constraint (14) in subproblem **Pv:**.

We can use the same manner to linearize the quadratic term in the objective (19) of subproblem **Pv**. We define parameter $\mu_a^p = \sum_{p' \in P/p} n_{p'} \times v_a^{p'}$ denotes the number of passengers excluding those in passenger group p that use arc a. Q is the constant term of the quadratic term in the objective (19). The definition of variable s_a is given in Equation (33), and the quadratic term is linearized by Equation (34). The detailed process to obtain Equation (34) is similar to that given in Equation (32), which is omitted.

$$s_a = \begin{cases} 0 & \mu_a^p \geq \sum_{k \in K} q_k \times \overline{x}_a^k \\ \sum_{k \in K} q_k \times \overline{x}_a^k - n_p \times v_a^p - \mu_a^p & \mu_a^p < \sum_{k \in K} q_k \times \overline{x}_a^k \end{cases} \tag{33}$$

$$(\sum_{p \in P} n_p \times v_a^p - \sum_{k \in K} q_k \times \overline{x}_a^k + s_a)^2 = \begin{cases} n_p \times (n_p - 2 \times \sum_{k \in K} q_k \times \overline{x}_a^k + 2 \times \mu_a^p) \times v_a^p + Q & \mu_a^p \geq \sum_{k \in K} q_k \times \overline{x}_a^k \\ 0 & \mu_a^p < \sum_{k \in K} q_k \times \overline{x}_a^k \end{cases} \tag{34}$$

From A.1 and A.2, we can find how to handle an inequity constraint in ADMM. However, in our problem, the capacity of trains is usually tightly occupied by passengers in a major disruption. Therefore, the number of passengers on a train tends to approximately equal the capacity of the train, which means that the function of the coupling inequity constraint (14) is similar to that of its equity form. Thus, cost coefficient $q_k \times (q_k + 2 \times \mu_a^k - 2 \times \sum_{p \in P} n_p \times \overline{v}_a^p)$ is used in Equation (20) to handle the quadratic term.

$$q_k \times (q_k + 2 \times \mu_a^k - 2 \times \sum_{p \in P} n_p \times \overline{v}_a^p) \begin{cases} > 0 & \text{If } q_k + 2 \times \mu_a^k > 2 \times \sum_{p \in P} n_p \times \overline{v}_a^p \\ = 0 & \text{If } q_k + 2 \times \mu_a^k = 2 \times \sum_{p \in P} n_p \times \overline{v}_a^p \\ < 0 & \text{If } q_k + 2 \times \mu_a^k < 2 \times \sum_{p \in P} n_p \times \overline{v}_a^p \end{cases} \tag{35}$$

From formula (35), we know that if the total capacity of trains on arc a is larger than the current passenger volume on the same arc a, the cost coefficient is a positive value, which denotes that a positive cost is added to this arc when a train wants to use it. Accordingly, trains are discouraged to apply arc a. If the total capacity of trains on arc a equals the current passenger volume on the same arc a, the cost coefficient is 0. However, if the total capacity of trains on arc a is smaller than the current passenger volume on the same arc a, the cost coefficient is negative, which denotes that more trains are attracted to use arc a. This cost coefficient reflects the real situation in a disruption.

Similarly, cost coefficient $n_p \times (n_p - 2 \times \sum_{k \in K} q_k \times \overline{x}_a^k + 2 \times \mu_a^p)$ is used in Equation (21) to handle the quadratic term. When $n_p + 2 \times \mu_a^p > 2 \times \sum_{k \in K} q_k \times \overline{x}_a^k$, the value of this cost coefficient is positive, which means that passengers are discouraged to use arc a. However, when $n_p + 2 \times \mu_a^p < 2 \times \sum_{k \in K} q_k \times \overline{x}_a^k$, the value of the cost coefficient is negative, which denotes that passengers are attracted to use arc a. The effect of this cost coefficient is reasonable for passenger shortest path searching in a disruption.

Appendix B

In the ADMM approach, the values of the parameters ρ_1 and ρ_2 for the quadratic penalty term affect both the solution quality and the convergence speed. Proper selection of parameter values not only contributes to the efficiency of convergence but also can improve the solution quality. We tested various values of parameter ρ_1. The upper bounds of the linear term (up_1) and the quadratic term (up_2) of ADMM for the coupling constraint were set to $0.3\rho_1$ and $0.6\rho_1$, respectively. The lower bounds of linear term (lo_1) and quadratic term (lo_2) of ADMM for the coupling constraint were set to -$0.3\rho_1$ and -$0.6\rho_1$, respectively. The value of parameter ρ_2 was set to 0.3. We limited the outer iteration to ten steps. The results are shown in Table 18 and Figure 15. In Table 18, we checked whether headway and station capacity constraint is violated in the current iteration with a certain value of ρ_1, and a tick indicates the violation exists.

Table 18: The sensitivity analysis of parameter ρ_1

Iterations	1	2	3	4	5	6	7	8	9	10
$\rho_1 = 30$	✓		✓	✓				✓		✓
$\rho_1 = 40$				✓	✓		✓			
$\rho_1 = 50$		✓		✓	✓		✓	✓	✓	✓
$\rho_1 = 60$										

From Table 18, we can see that when the value of parameter ρ_1 is relatively small, the headway and coupling constraints are violated in most iterations. With an increase in parameter ρ_1, fewer headway and coupling constraints are violated. Specifically, the headway and station capacity conflicts are eliminated when the value of ρ_1 is ≥ 30. Thus, we can always obtain a feasible disposition timetable for trains. However, a relatively large value of parameter ρ_1 may reduce the solution quality. The influence of parameter ρ_1 on the upper bound solution is shown in Figure 15. As expected, a better upper bound solution can generally be obtained with a relatively smaller value of parameter ρ_1. However, the upper bound solution with $\rho_1 = 30$ is not the best. This is probably because the solutions of many iterations are not feasible. The headway and station capacity constraints are still violated. Considering both the feasibility and quality of solutions, the best value of ρ_1 is 40 in our large case study.

When parameter ρ_1 is 40, we further investigated the influence of parameter ρ_2 on the solution. We tested various values of ρ_2 from 0.1 to 0.4 with an interval of 0.1. The best upper bound solutions obtained within ten outer iterations are shown in Figure 16. It can be seen that the solution converges best when parameter $\rho_2 = 0.2$ after iteration 7. The best upper bound obtained at iteration 10 is similar for $\rho_2 = 0.2$ and $\rho_2 = 0.3$. Therefore, the value of parameter ρ_2 should be 0.2 to enable rapid improvement of the convergence.

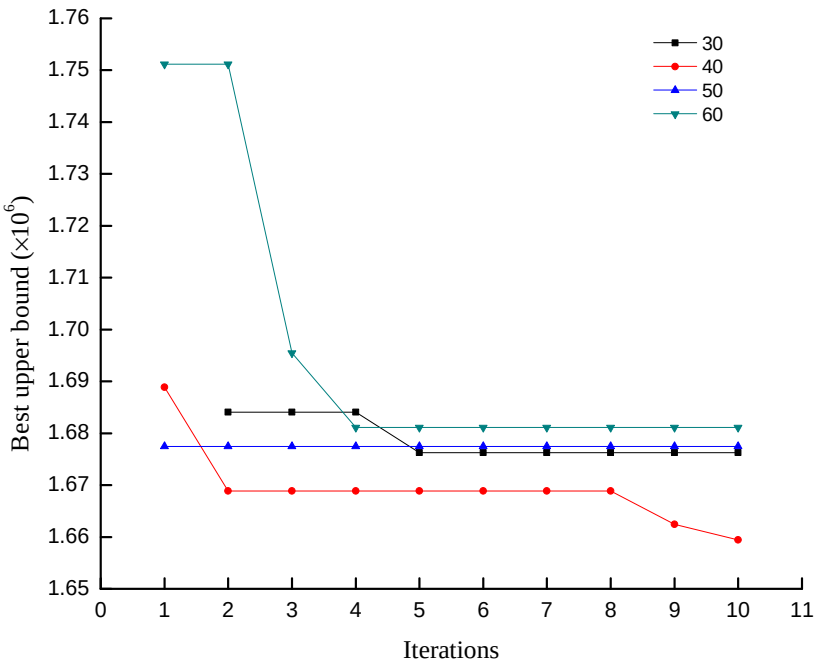

Figure 15: The upper bound solutions with various values of parameter ρ_1

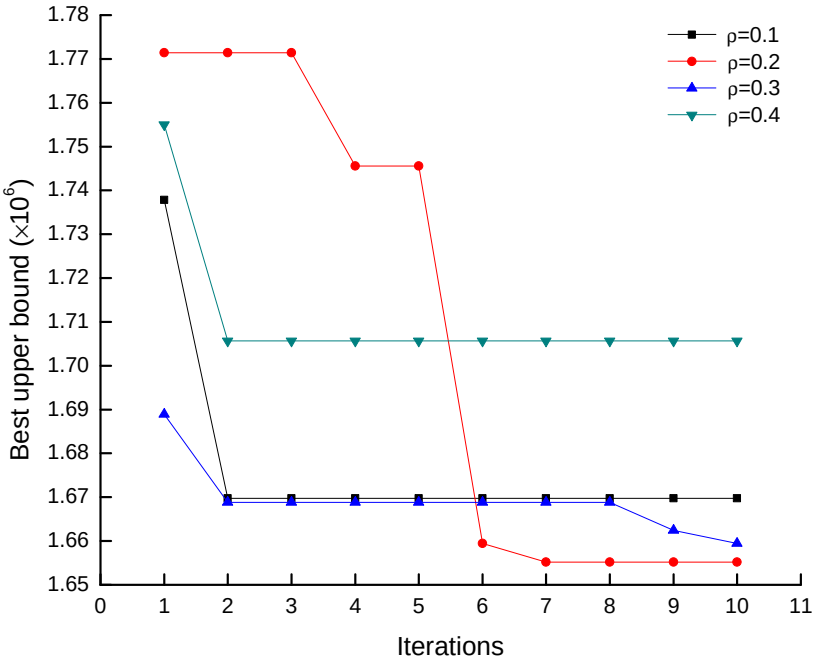

Figure 16: The upper bound solutions with various values of parameter ρ_2

Appendix C

Algorithm 2 The algorithm for solving subproblem **Px**

Input:

Space-time network for trains $G_{tr} = (E_{tr}, A_{tr})$;

The arc cost of space-time network for trains c_a^k;

Train set K;

The origin o_k and destination d_k, and originally start time e_k and finally arrival time l_k for each train $k \in K$;

Current Lagrangian multipliers $\gamma(a)$;

Current passenger routing results, the total number of passengers on each arc a, $\sum_{p \in P} n_p \times v_a^p$;

The maximum number of inner iterations Θ_t;

The disruption information, disrupted space-time train arc set A_{tr}^D

Output:

Train rescheduling results x_a^k

Step 1: Initialization

Initialize all train rescheduling variables $x_a^k = 0$;

Initialize Lagrangian multiplier $\xi(a)$ and penalty parameter ρ_1

Step 2: Train rescheduling

For each train k, perform Step 2.1 and Step 2.2

Step 2.1 Update train arc cost

Set the space-time train arc cost $c_a^k = \infty, \forall a \in A_{tr}^D$;

Update the space-time train arc cost by equation (20b)

Step 2.2 Find the shortest path

Find the shortest path from vertex (o_k, e_k) to $(d_k, \hat{T})$ by dynamic programming algorithm, and let $x_a^k = 1$ for arc a along the shortest path

Step 3: Train schedule update

For each train schedule update iteration $\theta < \Theta_t$:

For each train k, do Step 3.1, Step 3.2, and Step 3.3

Step 3.1 Delete

Reset variable $x_a^k = 0$ for train arc $a \in A_{tr}^k$

Step 3.2 Update train arc cost

Set the space-time train arc cost $c_a^k = \infty, \forall a \in A_{tr}^D$;

Update the space-time train arc cost by equation (20b)

Step 3.3 Find the shortest path

Find the shortest path from vertex (o_k, e_k) to $(d_k, \hat{T})$ by dynamic programming algorithm, and let $x_a^k = 1$ for arc a along the shortest path

Step 3.4: Update Lagrangian multiplier

Update Lagrangian multiplier $\xi(a)$ by the following equation:

$\xi(a)^{\theta+1} = \xi(a)^{\theta} + \rho_1 \times (\sum_{k \in K} \sum_{a' \in \Phi(a)} x_{a'}^k - 1)$

Step 3.5: Update iteration step

$\theta = \theta + 1$

Step 4: Output

Output train rescheduling variable x_a^k

Appendix D

Algorithm 3 The algorithm for solving subproblem **Pv**

Input:

Space-time network for passengers $G_{pa} = (E_{pa}, A_{pa})$;

The initial arc cost of space-time network for passengers c_a^p;

Passenger group set P;

The origin o'_p and destination d'_p, and original start time e'_p and final arrival time l'_p for each passenger group $p \in P$;

Current Lagrangian multipliers $\gamma(a)$;

Current train scheduling results, $\sum_{k \in K} x_a^k$, for each arc $a \in A_{pa} \cap A_{tr}$;

The disruption information, disrupted space-time passenger arc set A_{pa}^D

Output:

Passenger routing results v_a^p.

Step 1: Initialization

Initialize all passenger routing variables $v_a^p = 0$;

Set the space-time passenger arc cost $c_a^p = \infty, \forall a \in A_{pa}^D$;

Initialize general passenger arc cost $\overline{c}_a^p$ by Equation (21a);

Step 2: Passenger routing

For each passenger group $p \in P$:

Find the shortest path from vertex (o'_p, e'_p) to $(d'_p, \hat{T})$ by dynamic programming algorithm, and let $v_a^p = 1$ for arc a along the shortest path.

Step 3: Passenger rerouting

For each passenger route update iteration $\theta < \Theta_p$:

For each passenger group p, do Step 3.1, Step 3.2 and Step 3.3

Step 3.1 Delete

Reset variable $v_a^p = 0$ for passenger arc $a \in A_{pa}^p$

Step 3.2 Update passenger arc cost

Set the space-time passenger arc cost $c_a^p = \infty, \forall a \in A_{pa}^D$;

Update the space-time passenger arc cost by equation (21a)

Step 3.3 Find the shortest path

Find the shortest path from vertex (o'_p, e'_p) to $(d'_p, \hat{T})$ by dynamic programming algorithm, and let $v_a^p = 1$ for arc a along the shortest path.

Step 3.4: Update iteration step

$\theta = \theta + 1$

Step 4: Output

Output passenger routing variable v_a^p

Appendix E

Algorithm 4 The algorithm for obtaining the upper bound based on a feasible disposition timetable

Input:

Space-time network for passengers $G_{pa} = (E_{pa}, A_{pa})$;

The initial arc cost of space-time network for passengers c_a^p;

Passenger group set P, and the volume (n_p) for each passenger group $p \in P$;

The origin o'_p and destination d'_p, and original start time e'_p and final arrival time l'_p for each passenger group $p \in P$;

Feasible train scheduling results, x_a^k;

Train capacity q_k for each train $k \in K$

Output:

Feasible passenger routing results v_a^p.

Step 1: Initialization

Initialize all passenger routing variables $v_a^p = 0$;

Initialize total passenger volume on arc a, $\varphi(a) = 0, \forall a \in A_{pa} \cap A_{tr}$;

Step 2: Passenger routing

Order the passenger group $p \in P$ based on the rules explained below;

For each passenger group $p \in P$:

Step 2.1 Update arc cost

For each passenger arc $a \in A_{pa} \cap A_{tr}$, if $\varphi(a) + n_p > q_k$ or $\sum_{k \in K} x_a^k = 0$, set $c_a^p = \infty$.

Step 2.2 Routing passenger groups

Find the shortest path from vertex (o'_p, e'_p) to $(d'_p, \hat{T})$ by dynamic programming algorithm, and let $v_a^p = 1$ and $\varphi(a) = \varphi(a) + n_p$ for arc a along the shortest path.

Step 3: Output

Output passenger routing variable v_a^p for upper bound solution

In Step 2, we first order passenger groups according to three rules.

- Passenger groups that have booked trains running on the non-disrupted lines are denoted as first. That is, we place passenger groups traveling only on the Bengbu-Hefei inter-city line and Hefei-Nanjing high-speed line first.
- Passenger groups are ordered according to the departure time of their booked trains from the first station within the considered railway network.
- For passengers booked the same trains, we order them based on the length of the travel distance (long-distance OD first).

The first rule indicates that we give priority to passengers on the non-disrupted lines. This is reasonable in a railway system with seat reservation. In the second rule, we load passengers planning to depart earlier first, which is similar to the popular "first come, first served" strategy. In the last rule, we first load long-distance passengers, which is helpful for reducing the systematic influence of disruptions on passengers.

Step 2.1 ensures the feasibility of the passenger routing plan. Passengers can only use arc $a \in A_{pa} \cap A_{tr}$ when it is used by trains, and passengers on a train cannot exceed the total train capacity.

Appendix F

Algorithm 5 Dynamic programming algorithm to solve each single train-rescheduling problem

Input:

Space-time network for trains $G_{tr} = (E_{tr}, A_{tr})$;

The arc cost of space-time network for trains c_a^k;

The origin o_k and destination d_k, and original start time e_k and final arrival time l_k for each train $k \in K$;

Step 1: Initialization

For train $k = 1$ to $|K|$:

For physical link $(i, j) = 1$ to $|L|$: //$|L|$ is the total number of links

For time $t = e_k$ to l_k:

If $i = o_k$ and $t = e_k$:

$\nu_{i,t}^k = 0$; // $\nu_{i,t}^k$ is the label for train k at node (i, t)

Else:

$\nu_{i,t}^k = \infty$;

Set train node precedence $PN_{i,t} = -1$, time precedence $PT_{i,t} = -1$

End for

End for

End for

Step 2: Forward finding the best node on the shortest path

For train $k = 1$ to $|K|$:

For physical link $(i, j) = 1$ to $|L|$:

For time $t = e_k$ to l_k:

Derive feasible downstream point j' for j, and feasible downstream time t' for t;

Calculate the general cost $\bar{c}_{ij'tt'}$ of arc (i, j', t, t') according to Equation (20b);

If $\nu_{i,t}^k + \bar{c}_{ij'tt'} < \nu_{j',t'}^k$:

$\nu_{j',t'}^k = \nu_{i,t}^k + \bar{c}_{ij'tt'}$;

$PN_{j',t'} = i$, $PT_{j',t'} = t$

End if

End for

End for

End for

Step 3: Backtrack the shortest path

Step 3.1: Find the last space-time node of train k on its shortest path obtained by DP

Step 3.2: Backtrack from the last space-time node to the first space-time node of train k based on the precedence relationship

Step 3.3: Reverse the backward path and output the shortest-path and the corresponding cost

The procedure of DP used to solve the routing problem for a single passenger group is similar to that used to solve the rescheduling problem for a single train. Thus, we omit the DP algorithm used to solve the routing problem for a single passenger group here.

References

Bertsekas DP (1999) Nonlinear programming, 2nd edn. Athena Scientific

Binder S, Maknoon Y, Bierlaire M (2017a) Exogenous priority rules for the capacitated passenger assignment problem. Transportation Research Part B: Methodological 105:19 – 42

Binder S, Maknoon Y, Bierlaire M (2017b) The multi-objective railway timetable rescheduling problem. Transportation Research Part C: Emerging Technologies 78:78 – 94

Boyd S, Parikh N, Chu E, Peleato B, Eckstein J (2011) Distributed optimization and statistical learning via the alternating direction method of multipliers. Foundations and Trends in Machine Learning 3(1):1–122

Cacchiani V, Caprara A, Fischetti M (2012) A lagrangian heuristic for robustness, with an application to train timetabling. Transportation Science 46(1):124–133

Cacchiani V, Huisman D, Kidd MP, Kroon LG, Toth P, Veelenturf LP, Wagenaar JC (2014) An overview of recovery models and algorithms for real-time railway rescheduling. Transportation Research Part B: Methodological 63:15–37

Cadarso L, Marín Á, Maróti G (2013) Recovery of disruptions in rapid transit networks. Transportation Research Part E: Logistics and Transportation Review 53:15–33

Caprara A, Fischetti M, Toth P (2002) Modeling and solving the train timetabling problem. Operations Research 50(5):851–861

Chen C, He B, Ye Y, Yuan X (2016) The direct extension of ADMM for multi-block convex minimization problems is not necessarily convergent. Mathematical Programming 155(1):57–79

Corman F, Meng L (2015) A review of online dynamic models and algorithms for railway traffic management. IEEE Transactions on Intelligent Transportation Systems 16(3):1274–1284

Corman F, DAriano A, Pacciarelli D, Pranzo M (2009) Evaluation of green wave policy in real-time railway traffic management. Transportation Research Part C: Emerging Technologies 17(6):607–616

Corman F, DAriano A, Marra AD, Pacciarelli D, Samà M (2017) Integrating train scheduling and delay management in real-time railway traffic control. Transportation Research Part E: Logistics and Transportation Review 105:213–239

Dollevoet T, Huisman D, Kroon LG, Veelenturf LP, Wagenaar JC (2017) Application of an iterative framework for real-time railway rescheduling. Computers & Operations Research 78:203 – 217

Eckstein J, Bertsekas DP (1992) On the Douglas-Rachford splitting method and the proximal point algorithm for maximal monotone operators. Mathematical Programming 55(1):293–318

Fang W, Yang S, Yao X (2015) A survey on problem models and solution approaches to rescheduling in railway networks. IEEE Transactions on Intelligent Transportation Systems 16(6):2997–3016

Gabay D (1983) Applications of the method of multipliers to variational inequalities. In: Fortin M, Glowinski R (eds) Augmented Lagrangian Methods: Applications to the Numerical Solution of Boundary-Value Problems, NorthHolland, Amsterdam

Gao Y, Kroon L, Schmidt M, Yang L (2016) Rescheduling a metro line in an over-crowded situation after disruptions. Transportation Research Part B: Methodological 93:425 – 449

Ghaemi N, Goverde RMP, Cats O (2016) Railway disruption timetable: Short-turnings in case of complete blockage. In: IEEE International Conference on Intelligent Rail Transportation, pp 210–218

Ghaemi N, Cats O, Goverde RMP (2017) A microscopic model for optimal train short-turnings during complete blockages. Transportation Research Part B: Methodological 105(Supplement C):423 – 437

Ghaemi N, Cats O, Goverde RMP (2018) Macroscopic multiple-station short-turning model in case of complete railway blockages. Transportation Research Part C: Emerging Technologies 89:113 – 132

Hirai C, Kunimatsu T, Tomii N, Kondou S, Takaba M (2009) A train stop deployment planning algorithm using a petri-net-based modelling approach. Quarterly Report of RTRI 50(1):8–13

Jiang F, Cacchiani V, Toth P (2017) Train timetabling by skip-stop planning in highly congested lines. Transportation Research Part B: Methodological 104:149 – 174

Kecman P, Corman F, D'Ariano A, Goverde RMP (2013) Rescheduling models for railway traffic management in large-scale networks. Public Transport 5(1):95–123

Kroon LG, Maróti G, Nielsen LK (2015) Rescheduling of railway rolling stock with dynamic passenger flows. Transportation Science 49(2):165–184

Lamorgese L, Mannino C (2015) An exact decomposition approach for the real-time train dispatching problem. Operations Research 63(1):48–64

Lamorgese L, Mannino C, Piacentini M (2016) Optimal train dispatching by benders-like reformulation. Transportation Science 50(3):910–925

Lin T, Ma S, Zhang S (2015) On the global linear convergence of the ADMM with multiblock variables. SIAM Journal on Optimization 25(3):1478–1497

Louwerse I, Huisman D (2013) Adjusting a railway timetable in case of partial or complete blockades. European Journal of Operational Research 235(3):583–593

Mahmoudi M, Zhou X (2016) Finding optimal solutions for vehicle routing problem with pickup and delivery services with time windows: A dynamic programming approach based on statespacetime network representations. Transportation Research Part B: Methodological 89:19 – 42

Meng L, Zhou X (2011) Robust single-track train dispatching model under a dynamic and stochastic environment: a scenario-based rolling horizon solution approach. Transportation Research Part B: Methodological 45(7):1080–1102

Meng L, Zhou X (2014) Simultaneous train rerouting and rescheduling on an n-track network: A model reformulation with network-based cumulative flow variables. Transportation Research Part B: Methodological 67:208 – 234

Nielsen LK, Kroon LG, Maróti G (2012) A rolling horizon approach for disruption management of railway rolling stock. European Journal of Operational Research 220(2):496 – 509

Robenek T, Maknoon Y, Azadeh SS, Chen J, Bierlaire M (2016) Passenger centric train timetabling problem. Transportation Research Part B: Methodological 89:107 – 126

Saha A, Tewari A (2013) On the nonasymptotic convergence of cyclic coordinate descent methods. SIAM Journal on Optimization 23(1):576–601

Sun R, Hong M (2015) Improved iteration complexity bounds of cyclic block coordinate descent for convex problems. In: Cortes C, Lawrence ND, Lee DD, Sugiyama M, Garnett R (eds) Advances in Neural Information Processing Systems 28, Curran Associates, Inc., pp 1306–1314

Veelenturf LP, Kidd MP, Cacchiani V, Kroon LG, Toth P (2016) A railway timetable rescheduling approach for handling large-scale disruptions. Transportation Science 50(3):841–862

Veelenturf LP, Kroon LG, Maróti G (2017) Passenger oriented railway disruption management by adapting timetables and rolling stock schedules. Transportation Research Part C: Emerging Technologies 80:133 – 147

Wagenaar J, Kroon L, Fragkos I (2017) Rolling stock rescheduling in passenger railway transportation using deadheading trips and adjusted passenger demand. Transportation Research Part B: Methodological 101:140 – 161

Xu P, Corman F, Peng Q, Luan X (2017) A train rescheduling model integrating speed management during disruptions of high-speed traffic under a quasi-moving block system. Transportation Research Part B: Methodological 104:638–666

Yan S, Tseng CH (2002) A passenger demand model for airline flight scheduling and fleet routing. Computers & Operations Research 29(11):1559 – 1581

Yao Y, Zhu X, Dong H, Wu S, Wu H, Tong] LC, Zhou X (2019) ADMM-based problem decomposition scheme for vehicle routing problem with time windows. Transportation Research Part B: Methodological 129:156 – 174

Yin J, Tang T, Yang L, Gao Z, Ran B (2016) Energy-efficient metro train rescheduling with uncertain time-variant passenger demands: An approximate dynamic programming approach. Transportation Research Part B: Methodological 91:178 – 210

Zhan S, Kroon LG, Veelenturf LP, Wagenaar JC (2015) Real-time high-speed train rescheduling in case of a complete blockade. Transportation Research Part B: Methodological 78:182–201

Zhan S, Kroon LG, Zhao J, Peng Q (2016) A rolling horizon approach to the high speed train rescheduling problem in case of a partial segment blockage. Transportation Research Part E: Logistics and Transportation Review 95:32–61

Zhang Y, Peng Q, Yao Y, Zhang X, Zhou X (2019) Solving cyclic train timetabling problem through model reformulation: Extended time-space network construct and alternating direction method of multipliers methods. Transportation Research Part B: Methodological 128:344 – 379

Zhou L, Tong LC, Chen J, Tang J, Zhou X (2017) Joint optimization of high-speed train timetables and speed profiles: A unified modeling approach using space-time-speed grid networks. Transportation Research Part B: Methodological 97:157 – 181

Zhou W, Teng H (2016) Simultaneous passenger train routing and timetabling using an efficient train-based lagrangian relaxation decomposition. Transportation Research Part B: Methodological 94:409 – 439

Zhu Y, Goverde RMP (2019a) Dynamic passenger assignment for major railway disruptions considering information interventions. Networks and Spatial Economics 19(4):1249–1279

Zhu Y, Goverde RMP (2019b) Railway timetable rescheduling with flexible stopping and flexible short-turning during disruptions. Transportation Research Part B: Methodological 123:149 – 181